First of all, we appreciate the reviewer's comments and suggestions. In response to the reviewer's comments, we have made relevant revisions to the manuscript. Listed below are our answers and the changes made to the manuscript according to the questions and suggestions given by the reviewer. Each comment of the reviewer (in black) is listed and followed by our responses (in blue).

Referee Report

Lee et al., Examination of effects of aerosol on a pyroCb and their dependence on fire intensity and aerosol perturbation using a cloud-system resolving model, submitted to Atmos. Chem. Phys., 2019

General comments

The paper addresses the important question of aerosol effects on pyroCb impacts on UTLS water vapor and cirrus cloud area, both of which have substantial, but uncertain, radiative impacts. The authors conclude that microphysical processes (e.g. autoconversion) in pyroCbs associated with weak fires / surface heat fluxes are sensitive to smoke aerosol enhancements, and that such aerosols intensify convection, affecting UTLS water vapor and cirrus. On the other hand, pyroCbs from more intense fires are not very sensitive to smoke effects. Such understanding of UTLS water vapor and cirrus response to smoke is critical to better predicting future atmospheric response to fires, whose frequency and intensity continue to increase.

The contribution of the paper is that it extends a previous modeling study (Kablick et al., 2018) by testing the effects of a range of aerosol concentrations and surface heat fluxes in a cloud-system resolving model and thus is able to show the variation in sensitivity to aerosols of pyroCb UTLS impacts. The authors find that UTLS and cirrus clouds are increased by the presence of smoke for weak fires but not strong fires, and explain the causal mechanisms. In the future, these sensitivities / processes could be parameterized in climate models.

The simulation methodology and analysis are rigorous, and the introduction and conclusions are well-organized and logical. However, the results section is very wordy/lengthy and often unclear, so substantial efforts should be made to improve clarity/efficiency of the text, and some figures should be removed or moved to the SI. I recommend publication in ACP after major revisions.

Based on the reviewer's comments below and through authors' efforts, the result section is condensed by removing unnecessary text as a way of improving the readability of text. Some figures are removed, following the reviewer's and the other reviewer's comments. For details, see authors' responses below.

Specific comments

Main Text

I'm not familiar with the terminology "basic updrafts." Perhaps it should be "maximum" or "typical" "updraft speed"?

"Basic" is replaced with "typical". Also, the following is added:

(LL110-111 on p4)

For the simplicity of the term, in this study, “typical updraft speeds” are referred to as “typical updrafts”.

Line 80 “makes individual droplet smaller.” Please include references.

References are added.

Line 84 “the efficiency is proportional to the sizes.” Please include references.

References are added.

Line 87 “invigorates updrafts and associated convection.” Please include references.

A reference is added.

Line 114 Replace “confident information” with “more confident information than from a microphysics-parameterizing model.” There are no in-situ observations used in the study for model validation and the conclusions are drawn purely from model representations of microphysical processes. Additionally, the pyroCb case is idealized (no temporal variation in heat flux or interactions with the atmosphere). Therefore, the sensitivity tests provide useful but limited information.

The corresponding text is revised as follows:

(LL120-128 on p5)

These simulations are for a case of a pyroCb which is identical to that in Kablick et al. (2018), and performed by using a cloud-system resolving model (CSRM) which is able to resolve cloud-scale dynamic and thermodynamic processes. By resolving these processes that play a critical role in the development of clouds and their interactions with aerosols, we are able to obtain information on aerosol effects on the pyroCb development and its impacts the UTLS water vapor and cirrus clouds, and on associated dynamic and thermodynamic mechanisms. This information is likely to be more confident than that from a model that does not resolve but parameterize those cloud-scale processes.

Line 119 After “used by Kablick et al. (2018),” please add a brief explanation of the benefit of using a more sophisticated microphysical scheme.

The following is added:

(LL131-140 on p5)

Through extensive comparisons between various types of bin schemes and bulk schemes, Fan et al. (2012) and Khain et al. (2015) have concluded that the use of bin schemes is desirable for reasonable simulations of clouds, precipitation, and their interactions with aerosols. This is because the bin scheme explicitly predicts cloud-particle size distributions, while the bulk scheme prescribes those size distributions. The bin scheme also uses collection efficiencies and terminal velocities varying with varying cloud-particle sizes to emulate this variation in reality, while the bulk scheme in general uses fixed efficiencies and terminal velocities, which are not able to consider the variation of collection efficiencies and terminal velocities in reality. This makes the bin scheme more sophisticated than the bulk scheme.

Line 139 I suggest changing “CSRM” to “Modeling Framework.” Remember that ACP has a broader audience than the cloud modeling community.

Done.

Lines 197-199 Why were these CCN concentrations chosen? Please include references that they are typical values, e.g. for smoke plumes and background or urban areas.

The following is added:

(LL229-232 on p8)

These prescribed concentrations of aerosols are typically observed in fire spots and their background (Pruppacher and Klett, 1997; Seinfeld and Pandis, 1998; Reid et al., 1999; Andreae et al., 2004; Reid et al., 2005; Luderer et al., 2009).

Line 228 To shorten the paper, I suggest eliminating sentences that describe the contents of the figures, which is already contained in the figure legends, and replacing “in Figure X” etc. with “(Fig. X)” after the result is described. Change “In Figure 1, the observed cirrus cloud at the top of the pyroCb” to “The observed cirrus cloud at the top of the pyroCb (Fig. 1)”

We followed this suggestion except for situations where some description of figures and “in Figure x” are needed for the flow of text.

Line 238 Remove sentences on lines 238-240, and add “(Fig. 4)” at the end of line 241 after “cloud reflectivity fields.”

Done.

Lines 266-271 Condense to “Hence, the variation of fire intensity can be represented by variation of fire-induced surface latent and sensible heat fluxes. As a first step, the control run is repeated by reducing fire-induced surface latent and sensible heat fluxes by factors of 2 and 4. The first repeated run represents a case with medium fire intensity, while the second represents a case with weak fire intensity.”

Done.

Line 289 Redundant. Alter to: “can also be dependent on the magnitude of fire-induced increases in aerosol concentrations.”

Done.

Lines 294-302 What real-world situations do aerosol concentrations of 30000, 7500, 2000, and 1000 cm-3 represent? Please provide some context in the text.

The following is added:

(LL361-366 on p12-13)

The aerosol concentration of 30000 cm^{-3} over the fire spot corresponds to a situation when fire produces a larger concentration of aerosols than a typically observed range between 10000 and 20000 cm^{-3}, while the aerosol concentrations of 7500, 2000 and 1000 cm^{-3} over the fire spot corresponds to a situation when fire produces a lower concentration of aerosols than the typically observed range (Reid et al, 1999; Andreae et al, 2004; Reid et al, 2005; Luderer et al., 2009).

Results section: Lengthy and hard to follow. Please make an effort to condense the text, and summarize key results at the end of each section.

Done.

Line 307: Change to “Results from the control and low-aerosol runs”

Section “Results” itself includes sections for all the simulations. So, we created a new subsection 4.1 which is named “the control run and the low-aerosol run”

Lines 313-316 Change to “In this study, we expand upon the results of Kablick et al. (2018) by focusing on aerosol effects on pyroCb development and subsequent impacts on UTLS water vapor and cirrus clouds.”

Done.

Move sentence on lines 327-328 to the beginning of the paragraph starting on line 317.

Done.

Lines 330-332 Remove description of Table 2

Done.

Lines 332-333 Remove “In Figure 5 and Table 2”, and add “(Fig. 5 and Table 2)” at end of sentence

Done

Lines 336-340 Delete first three sentences of this paragraph.

Done.

Lines 345-350 Delete last two sentences of this paragraph.

Done.

Line 351 In what regions does 16 km correspond to the

UTLS? Please provide some context in the text.

We defined the UTLS as follows:

(LL384-393 on p13)

Regarding the UTLS, in this study, the upper troposphere is defined to be between ~ 9 km in altitude and the tropopause that is ~ 13 km in altitude; the equilibrium level where the buoyancy of a rising air parcel becomes zero above the level of free convection is considered to be the tropopause (Emanuel, 1994). Hence, the defined upper troposphere occupies around a quarter of the total vertical extent of the troposphere. The lower stratosphere is defined to be between the tropopause and an altitude which is 10 km above the tropopause. Hence, the UTLS is between ~9 km and ~23 km in this study. Considering that the stratosphere is between the tropopause and its top that is generally ~ 50 km in altitude, the defined lower stratosphere occupies around a quarter of the total vertical extent of the stratosphere.

Lines 367-369 What is the significance of increasing the vertical extent of water vapor from 14 to 16 km? Please explain in the text.

The following is added:

(LL415-424 on p14)

This means that air parcels that include water vapor and rise from below the tropopause overshoot the tropopause by ~ 3 km in the pyroCb, while those parcels in the background do so by ~ 1 km. This in turn implies that air parcels and associated updrafts in the pyroCb are stronger to reach higher altitudes before their demise in the stratosphere than those in the background. Those stronger air parcels enable water-vapor layers to be deepened in the lower stratosphere, which in turn enable the interception of longwave radiation by water vapor to occur over longer paths in the lower stratosphere. These longer paths and greater water-vapor mass over the paths both contribute to more interception of longwave radiation by water vapor in the UTLS over the pyroCb than in the background.

Lines 370-372 How is UTLS defined here? Please explain in the text.

The following is added:

(LL384-393 on p13)

Regarding the UTLS, in this study, the upper troposphere is defined to be between ~ 9 km in altitude and the tropopause that is ~ 13 km in altitude; the equilibrium level where the buoyancy of a rising air parcel becomes zero above the level of free convection is considered to be the tropopause (Emanuel, 1994). Hence, the defined upper troposphere occupies around a quarter of the total vertical extent of the troposphere. The lower stratosphere is defined to be between the tropopause and an altitude which is 10 km above the tropopause. Hence, the UTLS is between ~9 km and ~23 km in this study. Considering that the stratosphere is between the tropopause and its top that is generally ~ 50 km in altitude, the defined lower stratosphere occupies around a quarter of the total vertical extent of the stratosphere.

(LL402-403 on p14)

Henceforth, the UTLS water vapor means water vapor in a part of the UTLS at and above the tropopause.

(LL443-444 on p15)

Henceforth, the UTLS cirrus clouds mean those clouds in a part of the UTLS below the tropopause.

Line 375 How is tropopause defined here? Please explain in the text.

The following is added:

(LL385-387 on p13)

the equilibrium level where the buoyancy of a rising air parcel becomes zero above the level of free convection is considered to be the tropopause (Emanuel, 1994).

Lines 379-381 Alter to: “In addition to water vapor in the UTLS, ice crystals comprising cirrus clouds around the tropopause play an important role in the global radiation budget. To identify the impact of the pyroCb on cirrus clouds…”

This sentence is considered redundant and is removed, since this important role by cirrus clouds is already mentioned in introduction.

Line 409 Alter to: “The sensitivity of updrafts, water vapor, and cirrus clouds to aerosol loading in the pyroCb may be affected by fire intensity.”

Done.

Line 414 Change “In other words” to “Thus”.

Done.

Line 422 Change “just based on” to “to evaluate the”.

Done.

Line 426 Change “Updrafts and the UTLS water vapor and cirrus cloud” to “Effects of updrafts on UTLS water vapor and cirrus cloud”.

Done.

Lines 438-443 Condense/clarify to “Of interest is that the greatest percentage increase in updraft mass flux is in the case of weak fire (weak-low to weak runs), smallest in the case of strong fire (low-aerosol to control runs), and intermediate in the case of medium fire (medium-low to medium runs) (Figure 9 and Table 2).”

Done.

Lines 452-453 Alter to: “The percentage difference for medium (weak) fire intensity is obtained by replacing the control run with the medium (weak) run and the low-aerosol run with the medium-low (weak-low) run in Equation (1).”

Done.

Lines 454-456 Delete “The percentage difference… Equation (1).”

Done.

Lines 456-459 Alter to: “Associated with the greatest (smallest) increases in updraft mass fluxes, the percentage increases in water vapor and cloud-ice mass in the UTLS (Equation 1), are the greatest (smallest) in the case of weak (strong) fire (Figures 10 and 11 and Table 2).”

We changed text pointed out here as follows:

(LL512-514 on p17)

Associated with the greater increases in updraft mass fluxes, the percentage increases in the UTLS water vapor and cloud-ice mass (Equation 1) are greater in the case of weaker fire (Figures 5 and 6 and Table 2).

Lines 459-464 Delete “Figures 10 and 11 … intensity.”

Done.

Lines 473-476 Alter to: “The simulation period is divided into four sub-periods for this next analysis: period 1 (initial formation of the pyroCb) between 17:00 and 19:00 GMT on August 5th, period 2 between 19:00 and 21:00 GMT on August 5th and period 3 between 21:00 GMT and 23:00 GMT on August 5th (initial stages of cloud development), and period 4 between 23:00 GMT on August 5th and 12:00 GMT on August 6th (mature and decaying stages).”

Done.

Lines 476-479 Delete “The initial formation” to “the decaying stages.”

Done.

Lines 481-485 Combine/condense these two sentences

Done.

Line 505 Alter “weakens” to “decreases”

A phrase including “weakens” is considered redundant and is removed.

Lines 525-529 Change “reduces” to “decreases”

Done.

Lines 545-558 Move this discussion and accompanying figure to SI. Summarize the section.

The discussion part pointed out here is removed following the other reviewer’s comment. This section is summarized at its end.

Lines 598-601 Alter “aerosol chemical composition and aerosol” to “aerosol chemical composition. Aerosol …”

Following the other reviewer’s comment, the section including text pointed out here is shortened a lot. Associated with this, text pointed out here is removed.

Line 602 Alter to “aerosol composition (Rogers and Yau (1991))”

Text including this part pointed out here is removed during the process of shortening corresponding section following the other reviewer’s comment.

Line 607-655 This is a very long paragraph. Please divide it into multiple ones.

The corresponding paragraph is shortened a lot following this comment here and the other reviewer's comment.

Lines 663-666 Confusing. Delete "The concentration of … Figures 3 and 14;"

Done.

Line 668 Delete "Stated differently"

Done. Also, the following sentence is considered redundant and is removed.

Lines 676-681 Alter to "This contributes to a situation where the increment (the average minimum size with weak fire intensity minus that with strong fire intensity, 0.03 □m), among the low-aerosol, medium-low, and weak-low runs is similar to that among the control, medium, and weak runs during period 1 (Figure 14)."

Text pointed out here is removed during the process of shortening the corresponding section, following the other reviewer's comment.

Lines 683-685 Accordingly, the increase in the average minimum size with decreasing fire intensity reduces the number of aerosol particles that can be activated to droplets (Figure 14)."

Text pointed out here is removed during the process of shortening the corresponding section, following the other reviewer's comment.

Lines 698 and 700 Alter "varies" to "decreases"

Done.

Lines 741-742 Redundant. Remove "Autoconversion … proportional."

Done.

Lines 770-779 Remove "Remember … (Figure 15a)."

We removed text between line 770 and 775. However, we did not remove text between line 776 and 779, since information in this text was not given before.

Line 848 Alter to "establishing a positive feedback"

Done.

Line 876-877 Clarify to state what the effects are

We clarified that these effects are about effect of fire-produced aerosols as follows:

(LL717-718 on p24)

This leads to the greater overall effects of fire-produced aerosols on the UTLS water vapor and ice with weaker fire intensity.

930 Alter to “conclusions”

Done.

Lines 942-973 Divide this paragraph in two, one for each conclusion. (1) “This means that the role of fire-produced aerosols in water-vapor transport to the UTLS and the production of cirrus cloud in the pyroCb becomes more significant as fire intensity weakens.” (2) “This more significant role with weaker fire intensity is also robust to the variation of the fire-induced aerosol perturbation with the varying fire intensity unless the variation is very high.”

Done.

Figures and Tables
Which figures are essential to the main text and which could be moved to the SI? I suggest moving Figs. 3 and 13 to the SI. I also suggest eliminating Figs. 5-7, since the same information is contained in Figs. 9-11.

Done. Following the comment by the other reviewer, Figures 3 and 13 are also removed.

Figures w/ multiple lines (4-11): Use multiple line styles (e.g. dashed, dotted, solid). Current lines are difficult to distinguish when printed in grayscale.

There is no additional cost for color printing in ACP. Hence, all the figures will be published in colored form.

Change “over cloudy areas” to “in cloudy areas” and state altitude ranges first, e.g. “at all altitudes in cloudy areas”

Done.

Table 2: Remove sentence lines 1255-1260 “Note…”
Put equation in parentheses after “for each fire intensity ((polluted – clean)/clean x 100 (%))”

Done.

Table 3: “cirrus-cloud mass density between 9 and 13 km in cloudy areas, over the simulation period between 17:00 GMT on August 5th and 12:00 GMT on August 6th
The numbers in parentheses are the percentage differences: ($control$−30000 ($or\ control$−7500) - low−$aerosol$)/ low−$aerosol$)” (etc. for other equations)

Done.

Fig. 1: Bright white represents cirrus (anvil) at the top of the pyroCb, while the red circle marks the fire spot. Dark white represents smoke produced by the fire.

Done.

Fig. 2: The simulated fire spot (red circle) …
Eliminate “The red circle… “

Done.

Fig. 5: “Vertical distributions of the averaged updraft mass fluxes over cloudy areas (where the sum of liquid-water content (LWC) and ice-water content (IWC) is non-zero) over the simulation period between 17:00 GMT on August 5th and 12:00 GMT on August 6th in the control and low-aerosol runs.”

Done.

Fig. 6: Specify line colors

"Vertical distributions of average water-vapor mass density in the control and low-aerosol runs at altitudes above 13 km and over the simulation period between 17:00 GMT on August 5th and 12:00 GMT on August 6th. Colored lines represent the average values in cloudy grid columns (non-zero sum of liquid-water path (LWP) and ice-water path (IWP)) in the control and low-aerosol runs, while the black line represents those values in non- cloudy columns (zero sum of LWP and IWP) in the control run."

Done.

Fig. 7: "Vertical distributions of averaged cloud-ice mass density in cloudy areas (non- zero sum of liquid-water content (LWC) and ice-water content (IWC)) over the simulation period between 17:00 GMT on August 5th and 12:00 GMT on August 6th in the control and low-aerosol runs."

Done.

Fig. 8: "Same as Fig. 7, for averaged deposition rate."

Done.

Fig. 12: "the averaged CDNC, Rv, and LWC at all altitudes in cloudy areas, over the period between 17:00 and 19:00 GMT on August 5th."

Done.

Fig. 14: "Diagrammatic depiction of the varying minimum size of aerosol activation (see Section 4.1.2 for details) with varying fire intensity in the unimodal aerosol size distribution which is assumed in this study."

Figure 14 in the old manuscript is removed by following the comment by the other reviewer.

Eliminate: "The details of the varying minimum size are described in Section 4.1.2"

Figure 14 in the old manuscript is removed by following the comment by the other reviewer.

Eliminate or move to main text: "Here, the variation of the minimum size from Dcs to Dcw is identical to that from Dps to Dpw."

Figure 14 in the old manuscript is removed by following the comment by the other reviewer.

Fig. 15: "The average rates of condensation, deposition and cloud-liquid freezing at all altitudes in cloudy areas and over periods (a) 2, (b) 3 and (c) 4. In panel (a), the average autoconversion rates are additionally shown."

Done.

Fig. 16: "Time series of differences in the average values of variables related to aerosol- induced invigoration of convection, at all altitudes in cloudy areas

between the (a) control and low-aerosol runs for strong fire intensity, (b) medium and medium-low runs for medium fire intensity and (c) weak and weak-low runs for weak fire intensity."

Done.

Atmos. Chem. Phys. Discuss.,
https://doi.org/10.5194/acp-2019-524-RC2, 2019

Atmospheric Chemistry and Physics Discussions

Interactive comment on "Examination of effects of aerosols on a pyroCb and their dependence on fire intensity and aerosol perturbation using a cloud-system resolving model" *by* Seoung Soo Lee et al.

Anonymous Referee #2

Received and published: 17 August 2019

First of all, we appreciate the reviewer's comments and suggestions. In response to the reviewer's comments, we have made relevant revisions to the manuscript. Listed below are our answers and the changes made to the manuscript according to the questions and suggestions given by the reviewer. Each comment of the reviewer (in black) is listed and followed by our responses (in blue).

Review of: "Examination of effects of aerosol on a pyroCb and their dependence on fire intensity and aerosol perturbation using a cloud-system resolving model"

Authors: Seoung Soo Lee, George Kablick III Zhanqing Li

Recommend major revisions.

General comment:

This manuscript examines the impacts of fire intensity and aerosol concentration on the strength of convection, microphysics processes, and upper level moisture through simulations using spectral-bin microphysics. I find that much of the paper is not particularly novel since it's fairly well known as this point that aerosol effects tend to be muted with increasing strength of convection. However, details regarding the impacts on microphysics processes are insightful. I found the most novel portion of the paper to be the final result regarding the fact that when a weak fire produces weaker aerosol emissions, the results tend to be muted. I think the paper needs to focus more heavily on the more novel aspects of the work.

In general, the paper needs to be greatly shortened. It is far longer than a typical journal article and needs to be made more concise, particular since it's a follow-on study. There are many places in the paper where the language is too "wordy". Many sentences and statements are written in a way that is difficult to read and can get in the way of representing the scientific results. Examples are given below in the specific comments section of this review.

We, authors, revised the manuscript based on this comment particularly by focusing on shortening the manuscript. To shorten the manuscript, we removed unnecessary text and figures not only by the following comments below but also by our own decision.

Specific comments:

Title: The title is too long. You could remove "using a cloud-system resolving model".

Done.

1. Lines 63-64: The changes in cirrus clouds altering the radiation budget has become a true but very common motivating factor for cloud microphysics related research as it applies to climate change. Your main motivation here is that pyroCbs with high aerosol loading can change climate. However, pycoCbs are a subcategory of deep convection that comprises a very small percentage of actual deep convective storms and cirrus anvils. As such, I think you need to improve your motivating statements for this work.

The following is added:

(LL65-74 on p3)

The level of our understanding of impacts of pyroCbs on water vapor and cirrus clouds in the UTLS over the global scale is very low and studies to improve this

understanding has been going on (Fromm et al., 2010). However, this paper does not focus on these pyroCb impacts at the global scale. Instead, this paper aims to gain a process-level understanding of mechanisms that control impacts of individual pyroCbs on water vapor and cirrus clouds in the UTLS. The examination of these mechanisms can provide useful information to parameterize interactions among pyroCbs, water vapor and cirrus clouds in climate models. Hence, this examination can contribute to studies that try to improve our understanding of the global-scale impacts of pyroCbs on water vapor and cirrus clouds by using climate models.

2. Line 114: Here you state that using a CSRM allows you to have "confident information" on aerosol effects. I think this assumption is a bit premature given that you have not yet discussed the model you are using or the microphysics parameterization and its capabilities. Some microphysics schemes do not necessarily provide "confident information". Perhaps you should first offer some assessment of your choice of model schemes being used.

Text pointed out is revised as follows:

(LL120-140 on p5)

These simulations are for a case of a pyroCb which is identical to that in Kablick et al. (2018), and performed by using a cloud-system resolving model (CSRM) which is able to resolve cloud-scale dynamic and thermodynamic processes. By resolving these processes that play a critical role in the development of clouds and their interactions with aerosols, we are able to obtain information on aerosol effects on the pyroCb development and its impacts the UTLS water vapor and cirrus clouds, and on associated dynamic and thermodynamic mechanisms. This information is likely to be more confident than that from a model that does not resolve but parameterize those cloud-scale processes. The basic modeling methodology in this study is similar to that used by Kablick et al. (2018). However, this study uses a more sophisticated microphysical scheme, i.e., a bin scheme, rather than the two-moment bulk scheme used by Kablick et al. (2018). Through extensive comparisons between various types of bin schemes and bulk schemes, Fan et al. (2012) and Khain et al. (2015) have concluded that the use of bin schemes is desirable for reasonable simulations of clouds, precipitation, and their interactions with aerosols. This is because the bin scheme explicitly predicts cloud-particle size distributions, while the bulk scheme prescribes those size distributions. The bin scheme also uses collection efficiencies and terminal velocities varying with varying cloud-particle sizes to emulate this variation in reality, while the bulk scheme in general uses fixed efficiencies and terminal velocities, which are not able to consider the variation of collection efficiencies and terminal velocities in reality. This makes the bin scheme more sophisticated than the bulk scheme.

3. Introduction: The introduction appears quite short on references. Other work has been done on pyroCbs and several additional relevant papers should be referenced.

The following references are added:

Fromm, M., D. T. Lindsey, R. Servranckx, G. Yue, T. Trickl, R. Sica, P. Doucet, S. Godin-Beekmann, et al. (2010), The untold story of pyrocumulonimbus, B. Am. Meteorol. Soc., 91 (9), 1193, doi:10.1175/2010BAMS3004.1.

Peterson, D., M. Fromm, J. Solbrig, E. Hyer, M. Surratt, and J. Campbell (2017), Detection and inventory of intense pyroconvection in western North America using GOES-15 daytime infrared data, J. Appl. Meteorol. Clim., 56 (2), 471-493.

Pumphrey, H., M. Santee, N. Livesey, M. Schwartz, and W. Read (2011), Microwave Limb Sounder observations of biomass-burning products from the Australian bush fires of February 2009, Atmos. Chem. Phys. , 11 (13), 6285-6296.

4. Line 160: What is your size distribution of IN? You discuss this here but there's no other mention of heterogeneous ice nucleation in the paper that I recall seeing.

The following is added:

(LL251-258 on p9)

Those studies have indicated that in general, median aerosol diameter and standard deviation of the distribution range from ~0.01 to ~0.03 μm and from ~2.0 to ~2.2, respectively, for aerosols that act as CCN. By taking the approximate median value of each of these ranges, median aerosol diameter and standard deviation of the adopted unimodal distribution of aerosols as CCN are assumed to be 0.02 μm and 2.1, respectively, for the control run. Following Seinfeld and Pandis (1998) and Phillips et al. (2007), for aerosols that act as IN, median aerosol diameter and standard deviation of the unimodal distribution are assumed to be 0.1 μm and 1.6 that are typical values in the continent.

The heterogeneous ice nucleation is calculated by using temperature and supersaturation in addition to IN size distribution. This is reflected as follows:

(LL180-182 on p7)

In these parameterizations, contact, immersion, condensation-freezing, and deposition nucleation paths are all considered by taking into account the size distribution of IN, temperature and supersaturation.

5. Line 199: At 150/cm3 this seems overly clean for representing a continental type case. Can you justify your choice here?

Yes, it is rather low concentration for the continental type case. However, this concentration is frequently observed in remote continental sites including the forest site adopted in this study, according to Pruppacher and Klett (1997), Seinfeld and Pandis (1998), Reid et al. (1999), Andreae et al. (2004), Reid et al. (2005), Luderer et al. (2009). These references are included in text

6. Section 2: Please provide more description of how aerosols are treated in the model. Are they transported around the domain after initialization? Is there nucleation scav-

enging and precipitation scavenging? Does the fire continue to act as an aerosol source after initialization or do the initial aerosols just get depleted? Each of these effects can impact the interpretation of the results. A fire continually producing aerosols over time.

The following is added:

(LL263-274 on p9-10)

Aerosols are diffused and advected by air flow in clouds. After activation or captured by precipitating hydrometeors, aerosols are transported within hydrometeors and removed from the atmosphere once hydrometeors that contain aerosols reach the surface. It is assumed that in non-cloudy areas, aerosol size and spatial distributions are set to follow the background counterparts which are set at the first time step. In other words, once clouds disappear completely at any grid points, aerosol size distribution and number concentration at those points recover to the background counterparts. This assumption has been used by numerous CSRM studies and proven to simulate overall aerosol properties and their impacts on clouds and precipitation reasonably well (Morrison and Grabowski, 2011; Lebo and Morrison, 2014; Lee et al., 2016). This assumption means that a situation where fire continuously produces aerosols to maintain the initial background aerosol concentrations is adopted by this study.

7. Section 2: What data was used to initialize and nudge the simulations?

The following is added:

(LL197-205 on p7)

Balloon soundings of winds, temperature and dew-point temperature were obtained every 6 hours from Ft. Smith observation station, which is located near the forested site, as described in Kablick et al. (2018). The sounding data at 12:00 GMT on August 5th are used to prescribe the initial atmospheric condition. Using the sequential soundings, at each altitude, temperature and humidity tendencies are obtained. These tendencies represent the impacts of synoptic- or large-scale motion on temperature and humidity with the assumption that sounding data represent the synoptic conditions, following Grabowski et al. (1996), Krueger et al. (1999) and Lee et al. (2018). These tendencies are horizontally homogeneous and applied to the control run every time step by interpolation.

8. Line 235: Your assessment of "good agreement" between the model and satellite image is based on very little comparison. Can you provide more convincing evidence that these simulations are well representing this pyroCb event?

We made an additional comparison of cloud macro-physical properties, as represented by LWP, IWP, cloud-top and cloud-base heights, between the observation and the control run.

The following is added:

(LL284-297 on p10)

The averaged liquid-water path (LWP) over areas with non-zero LWP in the control run is 960 g m^{-2}, while the averaged ice-water path (IWP) over areas with non-zero IWP in the control run is 202 g m^{-2}. These simulated LWP and IWP are ~10 % different from the satellite-retrieved counterparts. In this study, for the calculation of LWP (IWP), we only considered droplets (ice crystals); drops with radii smaller (greater) than 20 μm are classified as droplets (raindrops). Stated differently, droplet mass but not rain mass is used to obtain liquid-water content (LWC) and LWP, and the mass of ice crystals but not the mass of snow aggregates, graupel and hail is used to obtain ice-water content (IWC) and IWP. The averaged cloud-top height and cloud-base height over the period between when the pyroCb forms and when the pyroCb disappears is 10.3 km and 3.6 km in the control run, respectively, and these simulated top and base heights are ~7% different from the satellite-retrieved counterparts. This indicates the overall cloud macro-physical structures, as represented by LWP, IWP, cloud-top and cloud-base heights, are simulated reasonably well as compared to the observation.

9. Lines 341-342: Experience has shown that what you choose as your lower threshold for averaging cloud water or LWP impacts the interpretation of the results. What do you consider the lower threshold given that models can provide very small numbers of LWP that are non-zero? Including tiny values of LWP in an average can impact trends in results.

In this study, all the LWP values which are not zero are considered for calculation related to LWP.

Stated differently, as long as LWP is greater than 0.00 g m^{-2}, LWP is considered for the averaging process. For the calculation of LWP, we need to obtain LWC and it is true that results can be dependent on how to set up the threshold for LWC. Note that when LWC is greater than the threshold value, the LWC is used to calculate LWP and the averaging process. To respond to this comment, we vary the LWC threshold from 0.0 g m^{-3} to 0.01 g m^{-3} through 0.005 g m^{-3}; note that The threshold value of 0.00 g m^{-3} is adopted by this study, and in addition to this threshold value of 0.00 g m^{-3}, the threshold values of 0.005 g m^{-3} and 0.01 g m^{-3} are also frequently adopted by previous studies for LWC and LWP calculations. We find that this variation of the LWC threshold does not change the qualitative nature of results in this study.

10. Lines 386-389: It seems to me that these two sentences about cloud-ice mass density are just stating that there is cloud-ice in the pyroCb and no cloud-ice outside of it. It seems unnecessary to state this since non-cloudy areas imply a lack of cloud/ice. Perhaps you can be clearer on what the intent is for these sentences.

The corresponding sentence is removed and related text is revised as follows:

(LL434-444 on p15)

The altitude of homogeneous freezing is at 9 km , so cirrus clouds which are composed of ice crystals (or cloud ice) only are between 9 km and 13 km. Between 9 km and 13 km, there are the presence of cloud ice and thus cirrus clouds in the control run, meaning that the pyroCb, which is simulated in the control run, produces cirrus clouds (Figure 6). The amount of cirrus clouds in the control run, as represented by the averaged cloud-ice mass density, ranges from 0.028 to 0.037 g m^{-3} between 9 km and 13 km (Figure 6). The averaged cloud-ice number concentration and cloud-ice size, as represented by its volume mean radius, between 9 km and 13 km ranges from 6 to 20 cm^{-3}, and from 10 to 20 micron, respectively. The altitudes between 9 km and 13 km correspond to a part of the UTLS below the troposphere. Henceforth, the UTLS cirrus clouds mean those clouds in a part of the UTLS below the tropopause.

11. Lines 390-391: What about considering homogeneous freezing? This process should be a major contributor to anvil ice mass and number concentration. I would expect ice numbers to be huge if a large portion of your aerosols are nucleated and transported aloft.

Ice numbers are shown as in our response to comment 12. To indicate the role of homogeneous freezing in ice number, the following is added:

(LL450-454 on p15)

However, mainly due to the larger aerosol concentrations, and associated greater homogeneous aerosol and droplet freezing, there is a large ~20-fold increase in cloud-ice number concentration and associated with this, there is a large ~2-fold decrease in cloud-ice size in the control run between 9 km and 13 km as compared to that in the low-aerosol run.

12. Section 4: This section should probably contain some discussion of changes to cirrus cloud ice crystal number concentration. There could be quite an enhancement in cirrus crystal sizes and number which can strongly impact cloud top albedo. Given your motivation factor regarding radiation and climate change, this would seem relevant.

The following is added:

(LL440-442 on p15)

The averaged cloud-ice number concentration and cloud-ice size, as represented by its volume mean radius, between 9 km and 13 km ranges from 6 to 20 cm^{-3}, and from 10 to 20 micron, respectively.

(LL450-454 on p15)

However, mainly due to the larger aerosol concentrations, and associated greater homogeneous aerosol and droplet freezing, there is a large ~20-fold increase in cloud-ice number concentration

and associated with this, there is a large ~2-fold decrease in cloud-ice size in the control run between 9 km and 13 km as compared to that in the low-aerosol run.

Line 439: You state “percentage increase in updrafts”? Are you referring to the number of updrafts or the updraft speed?

Here, percentage increase in updrafts means percentage increase in updraft mass fluxes. Since the updrafts mass flux is “updraft speed” times “air density”, and air density at each altitude does vary negligibly among simulations, differences in updraft mass fluxes are mostly explained by those in updraft speed. Hence, percentage increase in updraft mass fluxes means percentage increase in updraft speed with good confidence.

The corresponding text is revised as follows based on the comment here and the other reviewer’s comment:

(LL495-498 on p17)

Of interest is that the greatest percentage increase in updraft mass flux is in the case of weak fire (weak-low to weak runs), smallest in the case of strong fire (low-aerosol to control runs), and intermediate in the case of medium fire (medium-low to medium runs) (Figure 4 and Table 2).

The following is added:

(LL498-503 on p17)

Since the updrafts mass flux is updraft speed that is multiplied by air density, and air density at each altitude does vary negligibly among simulations, differences in updraft mass fluxes are mostly explained by those in updraft speed. Hence, it can be said that percentage differences in updraft mass fluxes mean percentage differences in updraft speed with good confidence.

13. Lines 462-467: This couple of sentences is an example where the main point could be made more concise.

Text pointed out here is revised as follows:

(LL512-514 on p17)

Associated with the greater increases in updraft mass fluxes, the percentage increases in the UTLS water vapor and cloud-ice mass (Equation 1) are greater in the case of weaker fire (Figures 5 and 6 and Table 2).

14. Section 4.1.2: This entire section needs to be re-written or removed. The discussion of (LWC/CNDC) is overtly long and could be greatly condensed. To this same point, figures 13 and 14 are not necessary. The discussion here refers to basic algebra that goes into unnecessary description for the anticipated audience.

This section is simplified as seen in the revised manuscript. However, following a comment by the other reviewer, summary is added at the end of this section about LWC, CDNC and R_v.

Further, the section on equilibrium supersaturation is also unnecessary; a very short refresher regarding supersaturation could be useful, but most of the potential readers do not need a full review of this. Referring to Rogers and Yao (1991) is adequate.

Following the comment here, the corresponding section is shortened.

15. Lines 743-746: This is an example that shows up numerous times where the lengthy wording interferes with reading the paper in a concise manner. Here you state, “are higher in the low-aerosol run than in the control run for strong fire intensity, in the medium-low run than in the medium run for medium fire intensity, and in the weak-low run than in the weak run for weak fire intensity. . .” This is very cumbersome to

read and needs to be written in a concise way. When you see this type of monotonic behavior, you can simply state. This type of writing shows up many times in the paper and this represents just one example. Please examine the full paper for areas that can be written more concisely.

Based on the comment here, we revised the manuscript in a concise way, particularly focusing on expressions similar to those pointed out here.

16. Lines 743-760: It seems here that you're stating that larger Rv = more autoconversion in lower aerosol runs, and then in the next sentence it seems to state reduced Rv = less autoconversion in higher aerosol runs. You don't need to state both of these. One of them implies that the other must be true.

We just want to clarify that in the next sentence which is pointed out by the reviewer here, we do not talk about "reduced Rv= less autoconversion in higher aerosol runs" as phrased by the reviewer here. In the sentence, we talk about the variation of Rv and autoconversion with varying fire intensity. Hence, the two sentences pointed out here deliver two different types of information.

17. Line 960: The use of "enhancing difference" seems awkward. Directly state what the difference is (increase? decrease?)

The enhancing is replaced with "increasing"

Examination of effects of aerosols on a pyroCb and their dependence on fire intensity and aerosol perturbation

Deleted: using a cloud-system resolving model

Seoung Soo Lee[1], George Kablick III[2,3], Zhanqing Li[2], Chang-Hoon Jung[4], Yong-Sang Choi[5]

[1]Research Foundation, San Jose State University, San Jose, California, USA

[2]Earth System Science Interdisciplinary Center, University of Maryland, College Park, Maryland, USA

[3]US Naval Research Laboratory, Washington, DC, USA

[4]Department of Health Management, Kyungin Women's University, Incheon, South Korea

[5]Department of Environmental Science and Engineering, Ewha Womans University, Seoul, South Korea

Abstract

This study investigates how a pyrocumulonimbus (pyroCb) event influences water vapor concentrations and cirrus cloud properties near the tropopause, specifically focusing on how fire-produced aerosols affect this role via a modeling framework. Results from a case study show that when observed fire intensity is high, there is an insignificant impact of fire-produced aerosols on the convective development of the pyroCb and associated changes in water vapor and the amount of cirrus cloud near the tropopause. However, as fire intensity weakens, effects of aerosols on microphysical variables and processes such as droplet size and autoconversion increase. Modeling results shown herein indicate that aerosol-induced invigoration of convection is significant for pyroCb with weak-intensity fires and associated weak surface heat fluxes. Thus, there is a greater aerosol effect on the transportation of water vapor to the upper troposphere and the production of cirrus cloud with weak-intensity fires, whereas these effects are muted with strong-intensity fires.

Deleted: ¶

Deleted: the

1. Introduction

Recent studies (e.g., Pumphrey et al., 2011; Kablick et al., 2018) have shown that pyrocumulonimbus (pyroCbs) can transport significant amounts of water vapor to the upper troposphere and the lower stratosphere (UTLS) and thus may play a role in seasonal UTLS water vapor budgets. Any change in water vapor in the UTLS has an exceptionally strong influence on the global radiation budget and thus Earth's climate (Solomon et al., 2010). PyroCbs involve and control cirrus clouds around their tops that reach the UTLS. Changes in cirrus clouds in the UTLS are known to have a strong influence on the global radiation budget (Solomon et al., 2010). The level of our understanding of impacts of pyroCbs on water vapor and cirrus clouds in the UTLS over the global scale is very low and studies to improve this understanding has been going on (Fromm et al., 2010). However, this paper does not focus on these pyroCb impacts at the global scale. Instead, this paper aims to gain a process-level understanding of mechanisms that control impacts of individual pyroCbs on water vapor and cirrus clouds in the UTLS. The examination of these mechanisms can provide useful information to parameterize interactions among pyroCbs, water vapor and cirrus clouds in climate models. Hence, this examination can contribute to studies that try to improve our understanding of the global-scale impacts of pyroCbs on water vapor and cirrus clouds by using climate models.

By definition, pyroCbs initiate over a fire, and the large surface energy release affects their dynamic, thermodynamic and microphysical development (Fromm et al., 2010; Peterson et al., 2017). The dynamics of these events has been shown to be mostly controlled by fire-induced latent and sensible heat fluxes at and near the surface. However, questions remain about what role the large concentration of cloud condensation nuclei (CCN) contained in smoke has on the vertical development and microphysical properties. Studies (e.g., Rosenfeld et al., 2008; Storer et al., 2010; Tao et al., 2012) have shown that aerosols affect cumulonimbus clouds, and this raises a possibility that fire-generated aerosols affect pyroCb development. As an example of aerosol impacts on cumulonimbus clouds, these studies have demonstrated that increases in aerosol loading can make the size of droplets (i.e., cloud-liquid particles) smaller. Individual aerosol particles act as seeds for the formation of droplets and thus increasing aerosol loading or increasing aerosol

Deleted: A r
Deleted: y by
Deleted: (
Deleted:)
Deleted: s
Deleted: have
Deleted: through which pyroCbs affect water vapor and cirrus clouds in the UTLS
Deleted: thus
Deleted: be a way of better understanding climate changes.¶

concentrations lead to more droplets formed. More droplets mean more competition among them for available water vapor needed for their condensational growth, and this more competition makes individual droplets smaller (Twomey, 1977; Albrecht, 1989). Aerosol-induced smaller sizes of droplets reduce the efficiency of the growth of cloud-liquid particles to raindrops via autoconversion that is a collection process among cloud-liquid particles for them to grow to be raindrops, given that the efficiency is proportional to the sizes (Pruppacher and Klett, 1978; Rogers and Yau, 1991). This reduced efficiency leads to less cloud liquid converted to rain. More cloud liquid is thus available for transport to places above the freezing level by updrafts. This eventually induces more freezing of cloud liquid, which enhances parcel buoyancy, and this enhancement invigorates updrafts and associated convection (Rosenfeld, 2008).

Compared to the research done on the role played by fire-generated heat fluxes in the development of pyroCbs and their effects on water vapor and cirrus clouds in the UTLS, the research on that role by fire-generated aerosols has been scarce. Motivated by this lack of understanding, this paper focuses on the role by those aerosols in the development of a pyroCb and its effects on water vapor and cirrus clouds in the UTLS. To examine that role, this study extends the previous modeling work that was described in Kablick et al. (2018). That modeling work compared effects of fire-generated heat fluxes on the development of a pyroCb and its impacts on the UTLS water vapor and cirrus clouds to those of fire-generated aerosols. In that comparison, those effects of fire-generated aerosols were shown to be negligible as compared to those effects of heat fluxes. However, aerosol effects on cloud development vary with cloud typical properties such as typical updraft speeds that are determined by environmental conditions (e.g., Khain et al., 2008; Lee et al., 2008; Tao et al., 2012). For the simplicity of the term, in this study, "typical updraft speeds" are referred to as "typical updrafts". Typical updrafts are determined by environmental instability as represented by convective available potential energy (CAPE). Lee et al. (2008) have shown that different clouds with different typical updrafts, which are due to different CAPE, show different sensitivity of cloud microphysical and thermodynamic development to aerosol concentration. Hence, it is hypothesized that aerosol effects on the pyroCb development and its impacts on the UTLS water vapor and cirrus clouds can vary depending on the intensity of the pyroCb typical updrafts.

Deleted: .

Deleted: basic

Deleted: basic updraft

Deleted: s

Deleted: Basic

Deleted: s

Deleted: basic

Deleted: t

Deleted: s

Deleted: the intensity of

Deleted: pyroCb basic updraft

Deleted: s

Based on this hypothesis, to examine the potential variation of aerosol effects on the pyroCb development and its impacts on the UTLS water vapor and cirrus clouds with the varying typical updrafts of pyroCbs, numerical simulations are performed. These simulations are for a case of a pyroCb which is identical to that in Kablick et al. (2018), and performed by using a cloud-system resolving model (CSRM) which is able to resolve cloud-scale dynamic and thermodynamic processes. By resolving these processes that play a critical role in the development of clouds and their interactions with aerosols, we are able to obtain information on aerosol effects on the pyroCb development and its impacts the UTLS water vapor and cirrus clouds, and on associated dynamic and thermodynamic mechanisms. This information is likely to be more confident than that from a model that does not resolve but parameterize those cloud-scale processes. The basic modeling methodology in this study is similar to that used by Kablick et al. (2018). However, this study uses a more sophisticated microphysical scheme, i.e., a bin scheme, rather than the two-moment bulk scheme used by Kablick et al. (2018). Through extensive comparisons between various types of bin schemes and bulk schemes, Fan et al. (2012) and Khain et al. (2015) have concluded that the use of bin schemes is desirable for reasonable simulations of clouds, precipitation, and their interactions with aerosols. This is because the bin scheme explicitly predicts cloud-particle size distributions, while the bulk scheme prescribes those size distributions. The bin scheme also uses collection efficiencies and terminal velocities varying with varying cloud-particle sizes to emulate this variation in reality, while the bulk scheme in general uses fixed efficiencies and terminal velocities, which are not able to consider the variation of collection efficiencies and terminal velocities in reality. This makes the bin scheme more sophisticated than the bulk scheme.

Note that Kablick et al. (2018) examined aerosol effects on the convective development of a specific pyroCb case study, simulating microphysical conditions, detrained water vapor mixing ratios, and cirrus cloud properties only considering a typical updraft framework. The present study expands upon that work by performing sensitivity simulations in which typical updrafts in the pyroCb are allowed to vary, enabling us to ascertain the dependence of those aerosol effects on typical updrafts. Note that CAPE, which determines typical updrafts in convective clouds, are strongly dependent on surface latent and sensible heat fluxes (e.g., Houze, 1993), and in the case of pyroCb these fluxes

Deleted: basic
Deleted: s
Deleted: ,
Deleted: and microphysical
Deleted: confident
Deleted: ,
Deleted: and microphysical
Deleted: basic
Deleted: basic
Deleted: s
Deleted: basic
Deleted: s
Deleted: basic
Deleted: s

are controlled by fire intensity. Hence, these sensitivity simulations in turn enable us to study the dependence of those aerosol effects on fire intensity. Here, we see that the pyroCb typical updrafts are controlled by fire intensity and thus the pyroCb typical updrafts are referred to as fire-driven updrafts, henceforth.

Aerosol effects on clouds are initiated by an increase in aerosol concentration, which can be caused by an increase in aerosol emission at and near the surface, and dependent on how much aerosol concentration increases, or on the magnitude of an increase in aerosol concentration, i.e., aerosol perturbation (e.g., Rosenfeld et al., 2008; Koren et al., 2012). This dependence has not been examined in Kablick et al. (2018) and this study examines this dependence by performing additional sensitivity simulations where the magnitude of aerosol perturbation varies.

2. Modeling framework

We use the Advanced Research Weather Research and Forecasting (ARW) model, a nonhydrostatic compressible model, as the CSRM. Prognostic microphysical variables are transported with a fifth-order monotonic advection scheme (Wang et al., 2009). Shortwave and longwave radiation parameterizations have been included in all simulations by adopting the Rapid Radiation Transfer Model (RRTM; Mlawer et al., 1997; Fouquart and Bonnel, 1980).

To represent the microphysical processes, the CSRM adopts a bin scheme based on the Hebrew University Cloud Model described by Khain et al. (2009). The bin scheme solves a system of kinetic equations for the size distribution functions of water drops, ice crystals (plate, columnar and branch types), snow aggregates, graupel and hail, as well as cloud condensation nuclei (CCN) and ice nuclei (IN). Each size distribution is represented by 33 mass doubling bins, i.e., the mass of a particle m_k in the kth bin is determined as $m_k = 2m_{k-1}$.

The cloud-droplet nucleation parameterization, which is based on Köhler theory, is used to represent cloud-droplet nucleation. Arbitrary aerosol mixing states and arbitrary aerosol size distributions can be fed to this parameterization. To represent heterogeneous ice-crystal nucleation, the parameterizations by Lohmann and Diehl (2006) and Möhler et

Deleted: basic
Deleted: s
Deleted: are
Deleted: basic
Deleted: s are
Deleted: s
Deleted: CSRM
Deleted:
Deleted:
Formatted: Font: Not Italic
Formatted: Font: Not Italic
Formatted: Font: Not Italic
Formatted: Font: Not Italic
Formatted: Font: Times New Roman, 12 pt

al. (2006) are used. In these parameterizations, contact, immersion, condensation-freezing, and deposition nucleation paths are all considered by taking into account the size distribution of IN, temperature and supersaturation. Homogeneous aerosol (or haze particle) and droplet freezing, based on the size distribution of droplets, is also considered following the theory developed by Koop et al. (2000).

3. Case description and simulations

3.1 Control run

The control run for an observed pyroCb case is performed over a forested site in the Canadian Northwest Territories (60.03° N, 115.45° W). Kablick et al. (2018) give details about the site and the pyroCb case. The control run is identical to the Full Simulation in Kablick et al. (2018) except for the different microphysical schemes between them; remember that this study uses a bin scheme, while Kablick et al. (2018) used a bulk scheme. The control run is performed for one day from 12:00 GMT on August 5th to 12:00 GMT on August 6th in 2014 and captures the initial, mature, and decaying stages of the pyroCb. Balloon soundings of winds, temperature and dew-point temperature were obtained every 6 hours from Ft. Smith observation station, which is located near the forested site, as described in Kablick et al. (2018). The sounding data at 12:00 GMT on August 5th are used to prescribe the initial atmospheric condition. Using the sequential soundings, at each altitude, temperature and humidity tendencies are obtained. These tendencies represent the impacts of synoptic- or large-scale motion on temperature and humidity with the assumption that sounding data represent the synoptic conditions, following Grabowski et al. (1996), Krueger et al. (1999) and Lee et al. (2017). These tendencies are horizontally homogeneous and applied to the control run every time step by interpolation. The control run is performed in a three dimensional domain with horizontal and vertical lengths of 300 km and 20 km, respectively. For the simulation, the horizontal resolution is 500 m and the vertical resolution is 200 m to resolve cloud dynamic and thermodynamic processes.

Figure 1 shows a satellite image of the observed pyroCb and the fire spot whose spatial length is ~ 40 km when it is about to advance into its mature stage. To emulate this in the

Commented [SSL1]: From my thesis.

Deleted: his simulation

Deleted: ,

Deleted: and microphysical

Deleted: In Figure 1, the red circle marks the fire spot whose spatial length is ~ 40 km.

simulation, at the center of the simulation domain, a fire spot with a diameter of 40 km is placed (Figure 2). In the fire spot, the surface latent and sensible heat fluxes are set at 1800 and 15000 W m^{-2}, respectively. In areas outside of the fire spot in the domain, the surface latent and sensible heat fluxes are set at 310 and 150 W m^{-2}, respectively. These surface heat-flux values follow the previous studies which are Trentmann et al. (2006) and Luderer et al. (2006) and adopt boreal forest emissions. Following Kablick et al. (2018), the surface heat-flux values are prescribed with no temporal variation and no consideration of interactions between heat fluxes and the atmosphere in the control run. Hence, the setup for the surface heat fluxes is idealized and this enables a better isolation of aerosol effects themselves on the pyroCb development and its impacts on the UTLS water vapor and cirrus clouds for the given surface heat fluxes by excluding effects of interactions between the surface heat fluxes and atmosphere on those development and impacts.

For the selected pyroCb case, aerosol properties that can be represented by aerosol chemical composition, size distribution and concentration are unknown. Hence, in the fire spot for the first time step, the concentration of aerosols acting as CCN is prescribed to be 15000 cm^{-3} in the planetary boundary layer (PBL), and decreases exponentially with height above the PBL top. Outside of the fire spot for the first time step, the concentration of aerosols acting as CCN is prescribed to be 150 cm^{-3} in the PBL and also decreases exponentially with height above this layer. These prescribed concentrations of aerosols are typically observed in fire spots and their background (Pruppacher and Klett, 1997; Seinfeld and Pandis, 1998; Reid et al., 1999; Andreae et al., 2004; Reid et al., 2005; Luderer et al., 2009).

For the control run, the other aerosol properties are assumed to follow typical values determined in previous studies. For example, Reid et al. (2005) have shown that aerosol mass produced by forest fires is generally composed of ~50-70% of organic-carbon (OC) compounds, ~5-10% of black-carbon (BC) material, and ~20-45% of inorganic species. Based on those results, the approximate median value of each chemical component percentage range is used in the control run. Aerosol particles are assumed to be composed of 60% OC, 8% BC, and 32% inorganic species. In the control run, OC is assumed to be water soluble and composed of (by mass) 18 % levoglucosan ($C_6H_{10}O_5$, density = 1600 kg m^{-3}, van't Hoff factor = 1), 41 % succinic acid ($C_4H_6O_4$, density = 1572 kg m^{-3}, van't

Deleted: as shown in

Formatted: Don't adjust right indent when grid is defined, Don't adjust space between Latin and Asian text, Don't adjust space between Asian text and numbers

Hoff factor = 3), and 41 % fulvic acid ($C_{33}H_{32}O_{19}$, density = 1500 kg m^{-3}, van't Hoff factor = 5) based on typically observed chemical composition of OC compounds over fire sites (Reid et al., 2005). In the control run, the inorganic species is assumed to be ammonium sulfate, a representative inorganic species associated with fires (Reid et al., 2005). This chemical composition taken for aerosol particles is assumed to be spatiotemporally unvarying in the control run. According to Reid et al. (2005), Knobelspiessel et al. (2011), and Lee et al. (2014), it is reasonable to assume that the initial aerosol size distribution follows the unimodal lognormal distribution in fire sites. Hence, the control run adopts the unimodal lognormal distribution as an initial aerosol size distribution. Those studies have indicated that in general, median aerosol diameter and standard deviation of the distribution range from ~0.01 to ~0.03 μm and from ~2.0 to ~2.2, respectively, for aerosols that act as CCN. By taking the approximate median value of each of these ranges, median aerosol diameter and standard deviation of the adopted unimodal distribution of aerosols as CCN are assumed to be 0.02 μm and 2.1, respectively, for the control run. Following Seinfeld and Pandis (1998) and Phillips et al. (2007), for aerosols that act as IN, median aerosol diameter and standard deviation of the unimodal distribution are assumed to be 0.1 μm and 1.6 that are typical values in the continent. For the control run, aerosol properties of IN and CCN are assumed to be identical except that at the first time step, median aerosol diameter and standard deviation of the size distribution between IN and CCN are different, and the IN concentration is 100 times lower than the CCN concentration based on a general difference in concentration between CCN and IN (Pruppacher and Klett, 1978). Aerosols are diffused and advected by air flow in clouds. After activation or captured by precipitating hydrometeors, aerosols are transported within hydrometeors and removed from the atmosphere once hydrometeors that contain aerosols reach the surface. It is assumed that in non-cloudy areas, aerosol size and spatial distributions are set to follow the background counterparts which are set at the first time step. In other words, once clouds disappear completely at any grid points, aerosol size distribution and number concentration at those points recover to the background counterparts. This assumption has been used by numerous CSRM studies and proven to simulate overall aerosol properties and their impacts on clouds and precipitation reasonably well (Morrison and Grabowski, 2011; Lebo and Morrison, 2014; Lee et al., 2016). This

Deleted: .

Deleted: The unimodal distribution, which is adopted by the simulation, in the PBL over the fire spot is shown in Figure 3 with log-scales for x- and y-axes.

Deleted: . This is

assumption means that a situation where fire continuously produces aerosols to maintain the initial background aerosol concentrations is adopted by this study.

The observed cirrus cloud at the top of the pyroCb is located to the northeast of the fire spot due to the northeastward winds at the altitude of the cirrus cloud (Figure 1). The cloud first formed around the fire spot. However, winds advected it northeastward. The extent of the observed cirrus cloud is ~100 km. Figure 2 shows the simulated field of cloud-ice mass density at a time that corresponds to the satellite image in Figure 1. This field in Figure 2 represents the simulated cirrus cloud in the control run. As observed, the simulated cirrus is located to the northeast of the fire spot and the extent of the simulated cirrus cloud is ~ 100 km. Hence, we see that there is good agreement in the morphology of the cirrus cloud between the observation and the simulation.

The averaged liquid-water path (LWP) over areas with non-zero LWP in the control run is 960 g m^{-2}, while the averaged ice-water path (IWP) over areas with non-zero IWP in the control run is 202 g m^{-2}. These simulated LWP and IWP are ~10 % different from the satellite-retrieved counterparts. In this study, for the calculation of LWP (IWP), we only considered droplets (ice crystals); drops with radii smaller (greater) than 20 μm are classified as droplets (raindrops). Stated differently, droplet mass but not rain mass is used to obtain liquid-water content (LWC) and LWP, and the mass of ice crystals but not the mass of snow aggregates, graupel and hail is used to obtain ice-water content (IWC) and IWP. The averaged cloud-top height and cloud-base height over the period between when the pyroCb forms and when the pyroCb disappears is 10.3 km and 3.6 km in the control run, respectively, and these simulated top and base heights are ~7% different from the satellite-retrieved counterparts. This indicates the overall cloud macro-physical structures, as represented by LWP, IWP, cloud-top and cloud-base heights, are simulated reasonably well as compared to the observation.

The details of the reflectivity field are given in Kablick et al. (2018). There is good agreement between observed and simulated cloud reflectivity fields for this study (Figure 3). The agreement in the observed and simulated cirrus cloud, cloud macro-physical and reflectivity fields demonstrates that the pyroCb-case simulation is reasonable.

3.2 Low-aerosol run

Formatted: Font: (Asian) Times New Roman

Deleted: In Figure 1,

Deleted: t

Deleted: at the top of the simulated pyroCb and

Deleted: is

Deleted:

Deleted:

Formatted: Superscript

Formatted: Superscript

Moved (insertion) [3]

Deleted: Stated differently, droplet mass but not rain mass is used to obtain LWC and the mass of ice crystals but not the mass of snow aggregates, graupel and hail is used to obtain IWC.¶

¶

Figure 4 shows the vertical distribution of the cloud reflectivity field in dBZ, which is observed by the Cloudsat and averaged over the Cloudsat path, and its simulated counterpart in the control run. T

Deleted: in

Deleted: and simulated

Deleted: and reflectivity

To see the role played by fire-generated aerosols in the development of the pyroCb and its effects on water vapor and cirrus clouds in the UTLS, we repeat the control run by reducing aerosol concentration in the fire spot from 15000 cm^{-3} to the background aerosol concentration (i.e., 150 cm^{-3}). This reduction removes fire-generated aerosols in the fire spot. The only difference is in aerosol concentration in the fire spot and there are no other differences in the simulation setup which is described in Section 3.1 between the control run and this repeated run. Hence, comparisons between the control run and this repeated run, which is referred to as the low-aerosol run, will identify the role played by fire-generated aerosols in the pyroCb development and its impacts on the UTLS water vapor and cirrus clouds. Here, the low-aerosol run is identical to the Low Aerosol Simulation in Kablick et al. (2018) except for the different microphysical schemes between them.

3.3 Additional runs

We examine the above-mentioned potential variation of effects of fire-generated aerosols on the pyroCb development and its impacts on the UTLS water vapor and cirrus clouds with varying fire intensity and associated fire-driven updrafts. For the examination, we repeat the control run by varying fire intensity. Remember that surface latent and sensible heat fluxes on which fire-driven updrafts in convective clouds are strongly dependent are controlled by fire intensity. Hence, the variation of fire intensity can be represented by the variation of fire-induced surface latent and sensible heat fluxes. As a first step, the control run is repeated by reducing fire-induced surface latent and sensible heat fluxes by factors of 2 and 4. The first repeated run represents a case with medium fire intensity, while the second repeated run represents a case with weak fire intensity. Relative to these repeated runs, the control run represents a case with strong fire intensity. Henceforth, the first repeated run is referred to as "the medium run" and the second repeated run is referred to as "the weak run". Then, to see effects of fire-generated aerosols on the pyroCb development and its impacts on the UTLS water vapor and cirrus clouds for each of those cases with different fire intensity, the medium run and the weak run are repeated with the identical initial aerosol concentration to that in the low-aerosol run. The repeated medium

Deleted: Hence, fire intensity can be represented by fire-induced surface latent and sensible heat fluxes and the variation of fire intensity in the repeated control run is accomplished by the variation of these fire-induced surface heat fluxes. As a first step for the examination, the control run is repeated by reducing fire-induced surface latent and sensible heat fluxes by a factor of 2. Then, the control run is repeated again by reducing these fluxes by a factor of 4. …

run and weak run are referred to as "the medium-low run" and "the weak-low run", respectively. The control run, the medium run, and the weak run are the polluted-scenario runs, while the low-aerosol run, the medium-low run, and the weak-low run are the clean-scenario runs. Comparisons between the medium run and the medium-low run and those between the weak run and the weak-low run isolate those effects of fire-generated aerosols for the case of medium fire intensity and the case of weak fire intensity, respectively. Comparisons between the control run and the low-aerosol run identify those aerosol effects for the case of strong fire intensity.

Effects of fire-generated aerosols on the pyroCb development and its impacts on the UTLS water vapor and cirrus clouds can also be dependent on the magnitude of fire-induced increases in aerosol concentrations or aerosol perturbation in a fire spot. Motivated by this, the previously described simulations are repeated by varying the magnitude of aerosol perturbation in the fire spot. To test the sensitivity of results to the magnitude of fire-induced aerosol perturbation, for each fire intensity, we repeat the polluted-scenario run by increasing and reducing the magnitude by a factor of 2 in the fire spot but not outside of the fire spot. These simulations with the increased magnitude have an aerosol concentration of 30000 cm^{-3} at the first time step over the fire spot in the PBL and are referred to as the control-30000 run, the medium-30000 run, and the weak-30000 run for strong, medium, and weak fire intensity, respectively. These simulations with the reduced magnitude have an aerosol concentration of 7500 cm^{-3} at the first time step over the fire spot in the PBL and are referred to as the control-7500 run, the medium-7500 run, and the weak-7500 run for strong, medium, and weak fire intensity, respectively. Motivated by the analysis described in Section 4.3, we additionally repeat the medium run and the weak run with aerosol concentrations of 2000 and 1000 cm^{-3} at the first time step over the fire spot in the PBL, respectively. The repeated medium (weak) run is referred to as the medium-2000 (the weak-1000) run. Table 1 summarizes the simulations.

The aerosol concentration of 30000 cm^{-3} over the fire spot corresponds to a situation when fire produces a larger concentration of aerosols than a typically observed range between 10000 and 20000 cm^{-3}, while the aerosol concentrations of 7500, 2000 and 1000 cm^{-3} over the fire spot corresponds to a situation when fire produces a lower concentration

Deleted: how large fire-induced increases in aerosol concentrations are or

Deleted: aerosol

Deleted:

Deleted: 2

Formatted: Superscript

Formatted: Superscript

Formatted: Superscript

of aerosols than the typically observed range (Reid et al, 1999; Andreae et al, 2004; Reid et al, 2005; Luderer et al., 2009).

4. Results

4.1 The control run and the low-aerosol run

Results from the control run and the low-aerosol run, which are equivalent to the Full Simulation and the Low Aerosol Simulation in Kablick et al. (2018), respectively, are described here. Kablick et al. (2018) mainly focused on comparisons themselves between aerosol effects and heat-flux effects on pyroCb development and its impacts on the UTLS water vapor and cirrus clouds. In this study, we expand upon the results of Kablick et al. (2018) by focusing on aerosol effects on pyroCb development and its subsequent impacts on the UTLS water vapor and cirrus clouds.

The updraft mass flux is one of the most representative variables that are indicative of the cloud dynamic intensity and the magnitude of convective invigoration. The updraft mass flux is averaged over the simulation period between 17:00 GMT on August 5th and 12:00 GMT on August 6th and 17:00 GMT on August 5th is a time around which the pyroCb starts to from (Figure 4).

Regarding the UTLS, in this study, the upper troposphere is defined to be between ~ 9 km in altitude and the tropopause that is ~ 13 km in altitude; the equilibrium level where the buoyancy of a rising air parcel becomes zero above the level of free convection is considered to be the tropopause (Emanuel, 1994). Hence, the defined upper troposphere occupies around a quarter of the total vertical extent of the troposphere. The lower stratosphere is defined to be between the tropopause and an altitude which is 10 km above the tropopause. Hence, the UTLS is between ~9 km and ~23 km in this study. Considering that the stratosphere is between the tropopause and its top that is generally ~ 50 km in altitude, the defined lower stratosphere occupies around a quarter of the total vertical extent of the stratosphere.

Deleted: ¶

Formatted: Font: (Asian) Malgun Gothic, 12 pt, Not Bold

Formatted: Indent: Left: 0.69", No bullets or numbering

Formatted: Outline numbered + Level: 2 + Numbering Style: 1, 2, 3, … + Start at: 1 + Alignment: Left + Aligned at: 0.69" + Indent at: 0.94"

Formatted: Font: 13 pt

Deleted: by providing additional details of the simulation results

Deleted: the impacts of pyroCb development on the UTLS water vapor and cirrus clouds, and

Moved (insertion) [1]

Deleted: Figure 5

Deleted: shows the vertical distributions of the averaged updraft mass fluxes over cloudy areas, i.e., areas where the sum of liquid-water content (LWC) and ice-water content (IWC) is non-zero, and

Deleted: in the control run and the low-aerosol run for the case of strong fire intensity

Deleted: .

Deleted: and 12:00 GMT on August 6th is the end of the simulation period…

Deleted: In this study, drops with radii smaller (greater) than 20 μm are classified as droplets (raindrops). For the calculation of LWC (IWC), we only considered droplets (ice crystals). Stated differently, droplet mass but not rain mass is used to obtain LWC and the mass of ice crystals but not the mass of snow aggregates, graupel and hail is used to obtain IWC.¶

Moved up [3]: Stated differently, droplet mass but not rain mass is used to obtain LWC and the mass of ice crystals but not the mass of snow aggregates, graupel and hail is used to obtain IWC.

Commented [SSL2]: Change this definition of the tropopause later on.

Updraft mass fluxes in the control run are only ~3% greater than those in the low-aerosol run (Figure 4 and Table 2). Given the hundredfold difference in aerosol loading over the fire spot between the runs, this 3% difference in updraft fluxes is negligibly small. The comparison between water-vapor mass density over the cloudy columns and that over non-cloudy columns in the control run demonstrates that there is a substantial increase in the amount of water vapor in a part of UTLS at and above the tropopause due to the pyroCb (Figure 5 and Table 2). There is about five times greater water-vapor mass over the cloudy columns that represent the pyroCb area than in the background outside the pyroCb area in the control run. Henceforth, the UTLS water vapor means water vapor in a part of the UTLS at and above the tropopause.

Updrafts in the pyroCb transport water vapor to the UTLS at and above the tropopause, which leads to the substantial increase in the amount of the UTLS water vapor over the pyroCb area. For the simulation period between 17:00 GMT on August 5th and 12:00 GMT on August 6th, the averaged water-vapor mass fluxes at the tropopause over cloudy and non-cloudy grid columns are 8.30×10^{-6} and 0.57×10^{-6} kg m^{-2} s^{-1}, respectively. Due to the presence of the pyroCb and associated updrafts in cloudy grid columns, there are substantial increases in water vapor fluxes at the tropopause over those cloudy grid columns as compared to those fluxes in the background over non-cloudy grid columns. This leads to the larger amount of the UTLS water vapor over the pyroCb than in the background outside the pyroCb or the pyroCb area in the control run. It is also shown that the vertical extent of water vapor is extended further up to ~ 16 km by the pyroCb as compared to the extent of ~14 km in the background (Figure 5). This means that air parcels that include water vapor and rise from below the tropopause overshoot the tropopause by ~ 3 km in the pyroCb, while those parcels in the background do so by ~ 1 km. This in turn implies that air parcels and associated updrafts in the pyroCb are stronger to reach higher altitudes before their demise in the stratosphere than those in the background. Those stronger air parcels enable water-vapor layers to be deepened in the lower stratosphere, which in turn enable the interception of longwave radiation by water vapor to occur over longer paths in the lower stratosphere. These longer paths and greater water-vapor mass over the paths both contribute to more interception of longwave radiation by water vapor in the UTLS over the pyroCb than in the background.

Moved up [1]: The updraft mass flux is one of the most representative variables that are indicative of the cloud dynamic intensity and the magnitude of convective invigoration.

Deleted: As seen in Figure 5, the control run and the low-aerosol run for strong fire intensity have similar updraft mass fluxes. Table 2 gives the averaged values of updraft mass fluxes over cloudy areas at all altitudes and over the simulation period between 17:00 GMT on August 5th and 12:00 GMT on August 6th for simulations. In Figure 5 and Table 2,

Deleted: u

Formatted: Indent: First line: 0"

Deleted: Water vapor around and above the tropopause or the UTLS plays an important role in the global radiation budget, thus garnering much attention from the climate-change community. Motivated by this, we examine the role played by the pyroCb in the UTLS water vapor. The vertical distributions of averaged water-vapor mass density around and above the tropopause (~ 13 km) are shown in Figure 6. The water-vapor mass density shown by colored lines in Figure 6 is averaged over cloudy grid columns that have the non-zero sum of liquid-water path (LWP) and ice-water path (IWP) and over the simulation period between 17:00 GMT on August 5th and 12:00 GMT on August 6th. For the calculation of LWP (IWP), we only considered droplets (ice crystals) as for the calculation of LWC (IWC). The black line in Figure 6 shows the average of water-vapor mass density over non-cloudy grid columns that have the zero sum of LWP and IWP and over the simulation period between 17:00 GMT on August 5th and 12:00 GMT on August 6th in the control run. This represents the background water-vapor mass density. Table 2 shows the averaged values of water-vapor mass density over altitudes between 13 and 16 km for simulations.¶
As seen in Figure 6, 16 km is an altitude to which the non-zero water-vapor mass density over cloudy columns extends.

Deleted: as shown in Figure 6 and Table 2

Deleted: the

Moved (insertion) [2]

Deleted: ¶
There is about five times greater water-vapor mass over the cloudy columns that represent the pyroCb area than in the background outside the pyroCb area in the control run.¶

Moved up [2]: There is about five times greater water-vapor mass columns that represent the pyroCb area than in the background outside the pyroCb area in the control run.¶

Deleted:

Deleted: water vapor in

Deleted: water vapor mass in

Deleted: the

Deleted: 6

Commented [SSL3]: Revise it later on

Similar to the situation with updraft mass fluxes, there is only a small (~2%) increase in the averaged mass of the UTLS water vapor in the control run as compared to that in the low-aerosol run for strong fire intensity (Figure 5 and Table 2). The small variation in updraft mass fluxes between the control run and the low-aerosol run results in a small variation in the transportation of water vapor to the UTLS at and above the tropopause, and the averaged water-vapor fluxes at the tropopause between these two simulations. These averaged fluxes are over cloudy columns for the simulation period between 17:00 GMT on August 5th and 12:00 GMT on August 6th. The averaged water-vapor fluxes vary from 8.30×10^{-6} kg m^{-2} s^{-1} in the control run to 8.21×10^{-6} kg m^{-2} s^{-1} in the low-aerosol run.

The altitude of homogeneous freezing is at 9 km , so cirrus clouds which are composed of ice crystals (or cloud ice) only are between 9 km and 13 km. Between 9 km and 13 km, there are the presence of cloud ice and thus cirrus clouds in the control run, meaning that the pyroCb, which is simulated in the control run, produces cirrus clouds (Figure 6). The amount of cirrus clouds in the control run, as represented by the averaged cloud-ice mass density, ranges from 0.028 to 0.037 g m^{-3} between 9 km and 13 km (Figure 6). The averaged cloud-ice number concentration and cloud-ice size, as represented by its volume mean radius, between 9 km and 13 km ranges from 6 to 20 cm^{-3}, and from 10 to 20 micron, respectively. The altitudes between 9 km and 13 km correspond to a part of the UTLS below the troposphere. Henceforth, the UTLS cirrus clouds mean those clouds in a part of the UTLS below the tropopause.

Updrafts in the pyroCb produce supersaturation, which leads to the generation of cloud-ice mass and associated cirrus clouds via deposition, the primary source of cloud-ice mass. Similar to the situation with updraft mass fluxes, comparisons between the control run and the low-aerosol run for strong fire intensity show that there is only a small increase (~4%) in the mass of the UTLS circus clouds in the control run as compared to that in the low-aerosol run (Figure 6 and Table 2). However, mainly due to the larger aerosol concentrations, and associated greater homogeneous aerosol and droplet freezing, there is a large ~20-fold increase in cloud-ice number concentration and associated with this, there is a large ~2-fold decrease in cloud-ice size in the control run between 9 km and 13 km as compared to that in the low-aerosol run. Due to the negligible variation of updraft mass fluxes, there are negligible variations of supersaturation and deposition between the

Deleted: mass in the UTLS,

Deleted: as shown in Figure 6 and Table 2,

Deleted: is

Deleted: also

Deleted:

Deleted: In addition to water vapor in the UTLS, cloud ice or ice crystals around the tropopause play an important role in the global radiation budget. These ice crystals comprise cirrus clouds. To identify the role played by the pyroCb in cirrus clouds, Figure 7 shows the averaged cloud-ice mass density over cloudy areas for the simulation period of 17:00 GMT on August 5th to 12:00 GMT on August 6th in the simulations.

Deleted: ~

Deleted: ~

Deleted: ~

Deleted: ~

Deleted: ~

Deleted: t

Deleted: in the control run is shown in Figure 7, and

Deleted: ~

Deleted: ~

Formatted: Superscript

Deleted: .

Deleted: In non-cloudy areas and in the clear sky background outside the pyroCb, cloud-ice mass density equals zero. Hence in the control run, the pyroCb increases cloud-ice mass density between ~0.028 to ~0.037 g m^{-3} over the background.

Deleted: cloud-ice

Deleted: particularly between 9 km and 13 km, as shown in Figure 7 and Table 2,

simulations (Figure 7), and thus a negligible variation of the mass of the UTLS cirrus clouds between the control run and the low-aerosol run. Mainly due to the variation of aerosol concentrations, there are significant variations of cloud-ice number concentration and size between the control run and the low-aerosol run.

In summary, the pyroCb and associated updrafts cause a substantial enhancement of the transportation of water vapor to the UTLS at and above the tropopause. They also produce cirrus clouds. The role, which is played by fire-generated aerosols and their effects on the pyroCb and its updrafts, in the enhancement of the transportation of water vapor to the UTLS at and above the tropopause, and in the production of the mass of the UTLS cirrus clouds is not significant for strong fire intensity.

4.2 Dependence of aerosol effects on fire intensity

Taking interest in the negligible sensitivity of updrafts and their impacts on the UTLS water vapor and the mass of the UTLS cirrus clouds to aerosol loading in the pyroCb, we raise a possibility that this sensitivity is affected by fire intensity. When fire-generated surface heat fluxes and fire intensity are increased, it is likely that in-cloud latent heat is also increased because a major source of in-cloud latent heating is surface heat flux. Therefore, the aerosol-induced perturbations of latent heating may be relatively small compared with large in-cloud latent heat contributed by surface fluxes with very intense burning. Thus, aerosol-induced increases in parcel buoyancy, updrafts and their impacts on water vapor and the amount of cirrus clouds are relatively small compared with the large buoyancy, strong fire-driven updrafts, produced by strong fire intensity and the associated large in-cloud latent heat, and their impacts on water vapor and the amount of cirrus clouds.

Considering that a major source of in-cloud latent heat is surface heat fluxes, when the fire-generated surface heat fluxes and the fire intensity are reduced, in-cloud latent heat is also likely to be smaller. Here, we are interested in how the magnitude of an aerosol-induced perturbation of latent heating for a pyroCb with weak fire intensity is compared to that with strong fire intensity. This is to evaluate the possibility that with background in-cloud latent heat varying with fire intensity, the relative magnitude of aerosol-induced perturbation of latent heat to surface flux-dominated latent heat may vary.

Deleted: as seen in

Deleted: 8

Deleted: cloud-ice mass

Deleted: . Figure 8 shows the vertical distributions of the averaged deposition rate over cloudy areas for the simulation period of 17:00 GMT on August 5th to 12:00 GMT on August 6th.

Deleted: 1

Deleted: The weak sensitivity of updrafts, water vapor, and cirrus clouds to aerosol loading in the pyroCb may be related to fire intensity…

Deleted:

Deleted: In other words

Deleted: and

Deleted: and

Deleted:

Deleted: .

Deleted: This is just based on

Deleted: a

4.2.1 Effects of Updrafts on the UTLS water vapor and cirrus clouds

The average updraft mass fluxes in the low-aerosol run, the medium-low run and the weak-low run as shown in Figure 4 represent fire-driven updrafts for strong, medium and weak fire intensity, respectively. Due to different fire intensity and associated CAPE, fire-driven updrafts vary between these runs. The variation of these fluxes between the clean-scenario run and the polluted-scenario run for each fire intensity is induced by fire-generated aerosols. All of the cases of weak, medium and strong fire intensity show aerosol-induced increases in updraft mass fluxes (Figure 4 and Table 2). Of interest is that the greatest percentage increase in updraft mass flux is in the case of weak fire (weak-low to weak runs), smallest in the case of strong fire (low-aerosol to control runs), and intermediate in the case of medium fire (medium-low to medium runs) (Figure 4 and Table 2). Since the updrafts mass flux is updraft speed that is multiplied by air density, and air density at each altitude does vary negligibly among simulations, differences in updraft mass fluxes are mostly explained by those in updraft speed. Hence, it can be said that percentage differences in updraft mass fluxes mean percentage differences in updraft speed with good confidence. Here, the percentage difference, including both the percentage increase and decrease, is the relative difference in the value of variables between the polluted-scenario run than the clean-scenario run for each fire intensity. This percentage difference for strong fire intensity is obtained as follows in this study:

$$\frac{The\ control\ run\ minus\ the\ low-aerosol\ run}{The\ low-aerosol\ run} \times 100\ (\%) \qquad (1)$$

The percentage difference for medium (weak) fire intensity is obtained by replacing the control run with the medium (weak) run, and the low-aerosol run with the medium-low (weak-low) run in Equation (1). Associated with the greater increases in updraft mass fluxes, the percentage increases in the UTLS water vapor and cloud-ice mass (Equation 1) are greater in the case of weaker fire (Figures 5 and 6 and Table 2).

Deleted: 1
Deleted: and
Deleted: Figure 9 shows the averaged updraft mass fluxes over cloudy areas at each altitude in the runs with different fire intensity for the simulation period of 17:00 GMT on August 5th to 12:00 GMT on August 6th. Here,
Deleted: t
Deleted: d
Deleted: the low-aerosol run and the control run for strong fire intensity, between the medium-low run and the medium run for medium fire intensity, and between the weak-low run and the weak run for weak fire intensity, respectively,
Deleted: As seen in Figure 9 and Table 2,
Deleted: a
Formatted: Font: (Asian) Malgun Gothic
Formatted: Font: (Asian) Malgun Gothic
Formatted: Font: (Asian) Malgun Gothic
Formatted: Font: (Asian) Malgun Gothic
Deleted: Of interest is that the percentage increase in updrafts in the case of weak fire from those in the weak-low run to those in the weak run is the greatest, while the percentage increase in the case of strong fire from updrafts in the low-aerosol run to those in the control run is the smallest. The percentage increase for the case of medium fire from updrafts in the medium-low run to those in the medium run is intermediate (Figure 9 and Table 2).
Deleted: between the control run and the low-aerosol run for strong fire intensity, between the medium run and the medium-low run for medium fire intensity or between the weak run and the weak-low run for weak fire intensity.
Deleted: The percentage difference for medium fire intensity is obtained by replacing the control run with the medium run and replacing the low-aerosol run with the medium-low run in Equation (1).
Deleted: The percentage difference for weak fire intensity is obtained by replacing the control run with the weak run and replacing the low-aerosol run with the weak-low run in Equation (1). Associated with those greatest increases in updraft mass fluxes, the percentage increases in water vapor and cloud-ice mass in the UTLS, which are calculated by Equation (1), are the greatest in the case of weak fire as seen in Figures 10 and 11 and Table 2. Figures 10 and 11 show the averaged water-vapor and cloud-ice mass density at each altitude, respectively, over cloudy areas for the simulation period of 17:00 GMT on August 5th to 12:00 GMT on August 6th in the runs with different fire intensity. Associated with those smallest increases in updraft mass fluxes, the percentage increases in water vapor and cloud-ice mass in the UTLS are the smallest in the case of strong fire as seen in Figures 10 and 11 and Table 2. Associated with the medium increase in updraft mass fluxes, the percentage increases in water vapor and cloud-ice mass in the UTLS are intermediary in the case of medium fire as compared to the cases of strong and weak fire (Figures 10 and 11 and Table 2).

In this section, we see that although fire-produced aerosols invigorate updrafts in in all three types of fire intensity, the invigoration-induced increases in the UTLS water vapor and cloud-ice mass gets larger as fire intensity weakens.

4.2.2 Volume mean radius of droplets (R_v)

a. Cloud droplet number concentration (CDNC) and LWC

The simulation period is divided into four sub-periods for this next analysis: period 1 (initial formation of the pyroCb) between 17:00 and 19:00 GMT on August 5th, period 2 between 19:00 and 21:00 GMT on August 5th, and period 3 between 21:00 GMT and 23:00 GMT on August 5th (initial stages of cloud development), and period 4 between 23:00 GMT on August 5th and 12:00 GMT on August 6th (mature and decaying stages). CDNC, which is averaged at all altitudes in cloudy areas and over period 1, decreases as the fire intensity and updrafts decrease (Figure 8). The control run, the medium run and the weak run have higher aerosol concentrations over the fire spot (Table 1), which lead to the much higher averaged CDNC than the low-aerosol run, the medium-low run, and the weak-low run, respectively. Increasing CDNC enhances competition among droplets for a given amount of water, which is available for the condensational growth of droplets, in a cloud. Enhanced competition eventually curbs the condensational growth and reduces droplet size, which is represented by R_v in this study. This explains why R_v, which is averaged at all altitudes in cloudy areas and over period 1, is smaller in the polluted-scenario run than in the clean-scenario run for each fire intensity (Figure 8). Of interest is that as fire intensity weakens, although the averaged CDNC reduces, which tends to lower the competition among droplets, the averaged R_v decreases not only among the polluted-scenario runs over the fire spot but also among the clean-scenario runs over the fire spot (Figure 8). This is because R_v is proportional to $(\frac{LWC}{CDNC})^{\frac{1}{3}}$. Here, LWC represents the given amount of water which is available for the condensational growth of droplets. This proportionality means that for a given CDNC, a decrease in LWC also causes R_v to decrease, i. e., a decrease in the available amount of water for the condensational growth with no changes in CDNC induces a decrease in R_v. LWC, which is averaged at all altitudes in cloudy areas and over period 1,

Deleted: 1

Formatted: Superscript

Deleted: The simulation period is divided into four sub-periods for this next analysis: period 1 between 17:00 and 19:00 GMT on August 5th, period 2 between 19:00 and 21:00 GMT on August 5th, period 3 between 21:00 GMT and 23:00 GMT on August 5th, and period 4 between 23:00 GMT on August 5th and 12:00 GMT on August 6th. The initial formation of the pyroCb corresponds with the beginning of period 1, and along with periods 2 and 3 correspond to the initial stages of cloud development, while period 4 corresponds to the mature and the decaying stages. As seen in Figure 12,

Formatted: Superscript

Deleted: over

Deleted: at all altitudes

Deleted: However, the control run, the medium run, and the weak run have the much higher averaged CDNC than the low-aerosol run, the medium-low run, and the weak-low run, respectively. Remember that …t
t

Deleted: t

Deleted: than the low-aerosol run, the medium-low run and the weak-low run, respectively, over the fire spot (Table 1).

Deleted: over

Deleted: at all altitudes

Deleted: the control run than in the low-aerosol run for strong fire intensity, in the medium run than in the medium-low run for medium fire intensity, and in the weak run than in the weak-low run for weak fire intensity, respectively

Deleted: , as seen in

Deleted: 12

Deleted: control run, the medium run and the weak run with higher aerosol concentrations

Deleted: low-aerosol run, the medium-low run and the weak-low run with lower aerosol concentrations

Deleted: as shown in

Deleted: 12

Deleted: As shown in Figure 12,

Deleted: over

Deleted: at all altitudes

also decreases with weakening fire intensity and updrafts not only among the polluted-scenario runs but also among the clean-scenario runs (Figure 8). Effects of LWC on R_v outweigh those of CDNC and this leads to the decrease in the averaged R_v with weakening fire intensity (Figure 8).

Using the averaged LWC and the averaged CDNC that are shown in Figure 8, it is found that $(\frac{LWC}{CDNC})^{\frac{1}{3}}$ varies by 1.50×10^{-5} kg from 3.50×10^{-5} kg in the control run for strong fire intensity to 2.00×10^{-5} kg in the weak run for weak fire intensity, while it varies by 9.80×10^{-6} kg from 1.03×10^{-4} kg in the low-aerosol run for strong fire intensity to 9.32×10^{-5} kg in the weak-low run for weak fire intensity. Associated with this, the averaged R_v shows a 47 % reduction from 3.20 μm in the control run to 1.70 μm in the weak run, and the averaged R_v shows a 10 % reduction from 7.75 μm in the low-aerosol run to 6.98 μm in the weak-low run during period 1 (Figure 8).

In summary, the simulated LWC, CDNC, their variation with varying fire intensity, and the functional relation between LWC, CDNC and R_v, which is $R_v \propto (\frac{LWC}{CDNC})^{\frac{1}{3}}$, leads to a situation where R_v reduce much more among the polluted-scenario runs than among the clean-scenario runs during the period with the initial formation of the pyroCb.

b. Equilibrium supersaturation

During period 1, as fire intensity weakens and updraft speed decreases, parcel equilibrium supersaturation, which is supersaturation when supersaturation in a rising air parcel stops to increase (Rogers and Yau, 1991), lowers and thus, the minimum size of activated aerosol particles increases not only among the clean-scenario runs but also among the polluted-scenario runs. Mostly due to greater aerosol concentrations, the averaged equilibrium supersaturation and the averaged associated minimum size of activated aerosol particles over areas with positive updraft speed and period 1, are lower and higher, respectively, in the polluted-scenario run than in the clean-scenario run for each fire intensity. Rogers and Yau (1991) have also shown that higher aerosol concentrations induce lower and higher equilibrium supersaturation and the averaged associated minimum size of activated aerosol particles, respectively.

Deleted: control run, the medium run and the weak run

Deleted: low-aerosol run, the medium-low run and the weak-low run…

Deleted: , which weakens as fire intensity weakens,

Deleted: as seen in

Deleted: 12

Deleted: Note that the averaged LWC in the control run is similar to that in the low-aerosol run for strong fire intensity, while the averaged LWC in the medium run is similar to that in the medium-low run for medium fire intensity. The averaged LWC in the weak run is also similar to that in the weak-low run for weak fire intensity. The averaged LWC reduces with weakening fire intensity from that in the control run to that in the weak run through that in the medium run during period 1 (Figure 12). This reduction is similar to the reduction in the averaged LWC from that in the low-aerosol run to that in the weak-low run through that in the medium-low run during period 1 (Figure 12). Considering this, the fact that the averaged CDNC is much higher in the control run than in the low-aerosol run leads to a situation where $(\frac{LWC}{CDNC})$, which is the base of $(\frac{LWC}{CDNC})^{\frac{1}{3}}$, and thus R_v are much smaller in the control run than in the low-aerosol run for strong fire intensity; the fact that the averaged CDNC is much higher in the medium run than in the medium-low run leads to a situation where $(\frac{LWC}{CDNC})$ and R_v are much smaller in the medium run than in the medium-low run for medium fire intensity; the fact that the averaged CDNC is much higher in the weak run than in the weak-low run leads to a situation where $(\frac{LWC}{CDNC})$ ... [1]

Deleted: 12

Deleted: $(\frac{LWC}{CDNC})$ is calculated. $(\frac{LWC}{CDNC})$ reduces from 4.27×10^{-14} kg ... [2]

Deleted: , as seen in Figure 12,

Deleted: n for strong fire intensity

Deleted: for weak intensity

Deleted: for strong intensity

Deleted: for weak intensity

Formatted: Subscript

Formatted: Font: 16 pt

Formatted: Subscript

Deleted: ¶ ... [3]

Deleted: During period 1 between 17:00 and 19:00 GMT on ... [4]

Deleted: for the identical initial aerosol concentration, the ... [5]

Deleted: n

Deleted: the low-aerosol run for strong fire intensity, the medium ... [6]

Deleted:

Deleted: the control run for strong fire intensity, the medium run ... [7]

Deleted: Also, during period 1, percentage differences in updraft ... [8]

Deleted: m

Deleted: differences in

Deleted: between the control run and the low-aerosol run, ... [9]

Deleted: control run than in the low-aerosol run for strong fire ... [10]

Deleted: .

The averaged equilibrium supersaturation reduces from 0.21% in the control run for strong fire intensity to 0.10% in the weak run for weak fire intensity. Associated with this, the averaged minimum size in diameter increases from 0.09 μm in the control run to 0.12 μm in the weak run over period 1. The averaged equilibrium supersaturation reduces from 0.55% in the low-aerosol run for strong fire intensity to 0.31% in the weak-low run for weak fire intensity. Associated with this, the averaged minimum size increases from 0.04 μm in the low-aerosol run to 0.07 μm in the weak-low run over period 1.

The increase in the minimum-activation size with weakening fire intensity occurs closer to the right tail of the assumed unimodal aerosol size distribution among the polluted-scenario runs than among the clean-scenario runs. A smaller portion of the total aerosol concentration is in the size range which is closer to the right tail of the assumed unimodal aerosol size distribution than that which is less close to the right tail as long as changes in the minimum size in these two size ranges are similar and these ranges are on the right-hand side of the aerosol distribution; most of aerosol activation occurs for aerosol sizes on the right-hand side of the distribution peak, here we are only concerned with the size ranges on the right-hand side. So, a similar increase in the averaged minimum-activation size for a weakened fire results in a smaller percentage reduction in the total activated aerosol concentration and thus CDNC among the polluted-scenario runs than among the clean-scenario runs during period 1. CDNC, which is averaged in cloudy areas and period 1, decreases by 8% from 850 cm^{-3} in the control run to 780 cm^{-3} in the weak run. The averaged CDNC decreases by 76% from 33 cm^{-3} in the low-aerosol run to 8 cm^{-3} in the weak-low run (Figure 8). This contributes to greater reduction in $(\frac{LWC}{CDNC})^{\frac{1}{3}}$ and thus R_v as fire intensity weakens among the polluted-scenario runs than among the clean-scenario runs during period 1. This is for a similar simulated LWC between the polluted-scenario run and the clean-scenario run for each fire intensity (Figure 8).

In summary, due to larger aerosol concentrations and associated lower equilibrium supersaturation, the variation of the number of activated aerosols with varying fire intensity and updrafts occurs in the aerosol size range that is closer to the right tail of the assumed aerosol size distribution in the polluted-scenario runs than in the clean-scenario runs. In the size range that is closer to the right tail of the size distribution, there is a smaller portion of aerosol concentrations and thus the smaller percentage variation of the number of

Formatted: Indent: First line: 0.08"

Deleted: Associated with this, as diagrammatically depicted in Figure 14, the increase in the averaged minimum size with weakening fire intensity and associated decreasing updraft speed and equilibrium supersaturation occurs in the size range that is closer to the right tail of the assumed unimodal aerosol size distribution among the control run, the medium run and the weak run than among the low-aerosol run, the medium-low run and the weak-low run. Figure 14 is the same as Figure 3 but with linear scales for x- and y-axes. In Figure 14, D_{cs} and D_{cw} represent the averaged minimum size in the low-aerosol run for strong fire intensity and in the weak-low run for weak fire intensity, respectively, while D_{ps} and D_{pw} represent the averaged minimum size in the control run for strong fire intensity and in the weak run for weak fire intensity, respectively.

Deleted: for strong fire intensity

Deleted: for weak fire intensity

Deleted: for strong fire intensity

Deleted: for weak fire intensity

Deleted: The aerosol distribution as depicted in Figure 14 represents the averaged form of the distribution over the simulation domain and period. This indicates that on average, the overall initial form of aerosol size distribution is well maintained over the domain and period, although aerosol concentration in each size bin of the distribution evolves with time and space. The above-described siz... [11]

Deleted: at

Deleted: t

Deleted: is

Deleted: the tail

Deleted: control run, the medium run and the weak run

Deleted:

Deleted: the low-aerosol run, the medium-low run and the weak ... [12]

Deleted:

Deleted: Recall that a

Deleted: large

Deleted: .

Deleted: control run, the medium run and the weak run

Deleted: the low-aerosol run, the medium-low run and the weak ... [13]

Deleted: As seen in Figure 12,

Deleted: over

Deleted: varies

Deleted: with strong fire intensity

Deleted: with weak fire intensity

Deleted: varies

Deleted: with strong fire intensity

Deleted: with weak fire intensity

Deleted: the control run, the medium run and the weak run

Deleted: low-aerosol run, the medium-low run and the weak-low ... [14]

Deleted:

Deleted: control run and the low-aerosol run for strong fire ... [15]

Deleted: The contribution is easily understood if we assume ... [16]

activated aerosols and CDNC in the polluted-scenario runs than in the clean-scenario runs. This smaller variation of CDNC aids the greater reduction in R_v among the polluted-scenario runs than among the clean-scenario runs via the relation of $R_v \propto (\frac{LWC}{CDNC})^{\frac{1}{3}}$, in the situation where LWC is similar between the polluted-scenario run and the clean-scenario run for each fire intensity.

4.2.3 Autoconversion, freezing, deposition and condensation

According to previous studies (e.g., Khairoutdinov and Kogan, 2000; Liu and Daum, 2004; Lee and Baik, 2017), autoconversion is proportional to the size of cloud droplets. This is explained by the fact that the efficiency of collection among droplets is proportional to droplet size (Pruppacher and Klett, 1978; Rogers and Yau, 1991). Due to the larger R_v during period 1, the subsequent autoconversion rates, which are averaged in cloudy areas and over period 2, are higher in the clean-scenario run than in the polluted-scenario run for each fire intensity (Figure 9a). Due to the larger absolute and percentage reduction in R_v, as described in Section 4.2.2, there is a larger absolute and percentage reduction in autoconversion rate among the polluted-scenario runs than among the clean-scenario runs with weakening fire intensity during period 2 (Figure 9a). The averaged autoconversion rates over period 2 reduce from 3.61×10^{-6} g m^{-3} s^{-1} in the control run with strong fire intensity to 0.93×10^{-6} g m^{-3} s^{-1} in the weak run with weak fire intensity through 2.01×10^{-6} g m^{-3} s^{-1} in the medium run with medium fire intensity by 74%. Those averaged autoconversion rates reduce from 4.52×10^{-6} g m^{-3} s^{-1} in the low-aerosol run with strong fire intensity to 3.94×10^{-6} g m^{-3} s^{-1} in the weak-low run with weak fire intensity through 4.43×10^{-6} g m^{-3} s^{-1} in the medium-low run with medium fire intensity by 14%. Associated with this, differences in the averaged autoconversion rates between the polluted-scenario run and the clean-scenario run get greater as fire intensity weakens during period 2 (Figure 9a).

Due to smaller autoconversion rates, there is more cloud liquid available for freezing in the polluted-scenario run than in the clean-scenario run for each fire intensity, particularly during period 2. Hence, the rate of cloud-liquid freezing, which is averaged in cloudy areas and period 2, is greater in the polluted-scenario run than in the clean-scenario

Deleted: 1

Deleted: strongly dependent on the size of cloud droplets and is

Deleted: Larger droplets collect or coalesce with other droplets more efficiently. Autoconversion is a collection process among droplets to form raindrops, which means autoconversion rate and cloud droplet size is proportional.

Deleted: over

Deleted: the low-aerosol run than in the control run for strong fire intensity, in the medium-low run than in the medium run for medium fire intensity, and in the weak-low run than in the weak run for weak fire intensity, respectively

Deleted: 15

Deleted: 1

Deleted: the control run, the medium run and the weak run

Deleted: the low-aerosol run, the medium-low run and the weak-low run …

Deleted: 15

Deleted: the weak run and the weak-low run for weak fire intensity are greater than those between the control run and the low-aerosol run for strong fire intensity over period 2; differences in the averaged autoconversion rates between the medium run and the medium-low run for medium fire intensity are greater than those between the control run and the low-aerosol run for strong fire intensity, and smaller than those between the weak run and the weak-low run for weak fire intensity

Deleted: 15

Deleted: the control run than in the low-aerosol run for strong fire intensity, in the medium run than in the medium-low run for medium fire intensity, and in the weak run than in the weak-low run for weak fire intensity, respectively

Deleted: over

run for each fire intensity (Figure 9a). Differences in autoconversion rates between the polluted-scenario run and the clean-scenario run, which increase with weakening fire intensity, induce those differences in the amount of cloud liquid available for freezing to get greater with weakening fire intensity (Figure 9a). Thus, differences in the averaged rate of cloud-liquid freezing between the polluted-scenario run and the clean-scenario run over period 2 gets greater with weakening fire intensity (Figure 9a). Due to this, differences in freezing-related latent heat between the runs increase with weakening fire intensity. When fire intensity is strong, the difference in freezing-related latent heat, which is averaged in cloudy areas and period 2, between the polluted-scenario run, which is the control run, and the clean-scenario run, which is the low-aerosol run, is 1.60×10^{-4} J m^{-3} s^{-1}. However, with medium fire intensity, that difference between the polluted-scenario run, which is the medium run, and the clean-scenario run, which is the medium-low run, is 6.98×10^{-4} J m^{-3} s^{-1}, while with weak fire intensity, that difference between the polluted-scenario run, which is the weak run, and the clean-scenario run, which is the weak-low run, is 7.94×10^{-4} J m^{-3} s^{-1}. This corresponds to the variation of the percentage differences, which are calculated by Equation (1), in the averaged freezing-related latent heat between the polluted-scenario run and the clean-scenario run from 9% with strong fire intensity to 83% with weak fire intensity through 51% with medium fire intensity over the period 2.

As shown in Lee et al. (2017), enhanced freezing-related latent heat strengthens updrafts in places where freezing occurs and this, in turn, enhances deposition and deposition-related latent heat. Hence, although deposition, which is averaged in cloudy areas and period 2, is slightly lower, due to those strengthened updrafts, the averaged deposition and deposition-related latent heat are greater in the polluted-scenario run than in the clean-scenario run for each fire intensity during period 3 (Figures 9a and 9b). Differences in the averaged freezing rate (and thus the averaged freezing-related latent heating) in cloudy areas between the polluted-scenario run and the clean-scenario run for each fire intensity do not change much up to ~20:30 GMT after they start to appear around 18:30 GMT (Figure 10). However, after ~20:30 GMT, these differences start to increase as time goes by for each fire intensity. This is because as convection intensifies, the transportation of cloud liquid to places above the freezing level starts to be effective around 20:30 GMT.

Deleted: control run than in the low-aerosol run, in the medium run than in the medium-low run, and in the weak run than in the weak-low run, respectively

Deleted: 15

Deleted: Remember that the control run for strong fire intensity, the medium run for medium fire intensity and the weak run for weak fire intensity constitute the polluted-scenario runs with higher aerosol concentrations over the fire spot, and the low-aerosol run for strong fire intensity, the medium-low run for medium fire intensity and the weak-low run for weak fire intensity constitute the clean-scenario runs with lower aerosol concentrations over the fire spot.

Deleted: 15

Deleted: 15

Deleted: over

Deleted: over

Deleted: control run than in the low-aerosol run for strong fire intensity, in the medium run than in the medium-low run for medium fire intensity, and in the weak run than in the weak-low run for weak fire intensity, respectively,

Deleted: 15

Deleted: 15

Deleted: As seen in Figure 16,

Deleted: d

Deleted: over

Deleted: the control run and the low-aerosol run for strong fire intensity, between the medium run and the medium-low run for medium fire intensity, and between the weak run and the weak-low run for weak fire intensity, respectively,

The greater freezing and thus freezing-related latent heat in the polluted-scenario run than in the clean-scenario run for each fire intensity, which start to be significant around 20:30 GMT as compared to those before 20:30 GMT, invigorates updrafts, which are represented by the averaged updraft mass fluxes in cloud areas. This subsequently causes updrafts to be stronger in the polluted-scenario run than in the clean-scenario run for each fire intensity from ~21:00 GMT on (Figure 10). Then, the stronger updrafts induce deposition, which is averaged in cloudy areas, to be greater in the polluted-scenario run than in the clean-scenario run for each fire intensity. This is around 10-20 minutes after the stronger updrafts in the polluted-scenario run than in the clean-scenario run for each fire intensity start to occur (Figure 10). Note that deposition-related latent heat is about one order of magnitude greater than freezing-related latent heat for a unit of mass of hydrometeors involved in phase-transition processes. This contributes to much greater differences in deposition-related latent heat during period 3 than those in freezing-related latent heat between the polluted-scenario run and the clean-scenario run for each fire intensity during period 2 or 3 (Figures 9a and 9b).

To satisfy mass conservation, the enhanced updrafts above the freezing level, due to enhanced freezing and deposition, induce more updraft mass fluxes below the freezing level in polluted-scenario run than in the clean-scenario run for each fire intensity. This leads to more convergence around and below cloud base, which is air flow from environment to cloud, in the polluted-scenario run than in the clean-scenario run for each fire intensity. The more mass fluxes and the more convergence below the freezing level, in turn, enhance condensation. Hence, condensation, which is averaged in cloud areas, starts to be greater when time reaches ~22:30 GMT in the polluted-scenario run than in the clean-scenario run for each fire intensity (Figure 10). This induces the averaged condensation and condensation-related latent heat to be greater in the polluted-scenario run than in the clean-scenario run for each fire intensity during period 4 (Figure 9c). Enhanced condensation in turn enhances updrafts, establishing a positive feedback between freezing, deposition, condensation, and updrafts and thus, enhancing freezing, deposition, condensation, and updrafts further. This enhancement due to feedback eventually determines the overall differences in the pyroCb properties and their impacts on the UTLS

Deleted: control run than in the low-aerosol run, in the medium run than in the medium-low run, and in the weak run than in the weak-low run, respectively

Deleted: over

Deleted: control run than in the low-aerosol run for strong fire intensity, in the medium run than in the medium-low run for medium fire intensity, and in the weak run than in the weak-low run for weak fire intensity, respectively,

Deleted: 6

Deleted: over

Deleted: the control run than in the low-aerosol run for strong fire intensity, in the medium run than in the medium-low run for medium fire intensity, and in the weak run than in the weak-low run for weak fire intensity, respectively.

Deleted: the control run than in the low-aerosol run, in the medium run than in the medium-low run, and in the weak run than in the weak-low run, respectively,

Deleted: 6

Deleted: the control run and the low-aerosol run for strong fire intensity, between the medium run and the medium-low run for medium fire intensity, and between the weak run and the weak-low run for weak fire intensity, respectively,

Deleted: s

Deleted: 15

Deleted: 15

Deleted: the control run than in the low-aerosol run for strong fire intensity, in the medium run than in the medium-low run for medium fire intensity, and in the weak run than in the weak-low run for weak fire intensity, respectively.

Deleted: control run than in the low-aerosol run for strong fire intensity, in the medium run than in the medium-low run for medium fire intensity, and in the weak run than in the weak-low run for weak fire intensity, respectively

Deleted: over

Deleted: the control run than in the low-aerosol run for strong fire intensity, in the medium run than in the medium-low run for medium fire intensity, and in the weak run than in the weak-low run for weak fire intensity, respectively

Deleted: 6

Deleted: control run than in the low-aerosol run for strong fire intensity, in the medium run than in the medium-low run for medium fire intensity, and in the weak run than in the weak-low run for weak fire intensity, respectively,

Deleted: 15

water vapor and cloud ice between the polluted-scenario run than in the clean-scenario run for each fire intensity.

Differences in freezing-related latent heat between the polluted-scenario run and the clean-scenario run increase with weakening fire intensity, particularly during period 2. Thus, percentage differences in freezing-affected updrafts and subsequently in deposition-related latent heat, which is averaged in cloudy areas and over period 3, between the polluted-scenario run and the clean-scenario run also increase with weakening fire intensity (Figures 9a, 9b and 10). Those differences, as calculated by Equation (1), in deposition-related latent heat are 16%, 181%, and 417 % for strong, medium, and weak fire intensity, respectively (Figures 9b and 10). Since percentage increases in deposition-related latent heat in the polluted-scenario run get greater with weakening fire intensity, the subsequent percentage increases in updrafts in the polluted-scenario run as compared to updrafts in the clean-scenario run get greater with weakening fire intensity, particularly during period 3 (Figure 10). During period 4, due to these greater increases in updrafts in the polluted-scenario run with weaker fire intensity, the percentage increases in condensation in the polluted-scenario run as compared to condensation in the clean-scenario run get greater with weakening fire intensity (Figures 9c and 10). Then, the increases in condensation, in turn, further enhance the increases in updrafts in the polluted-scenario run for each fire intensity. This enhancement is greater with weaker fire intensity due to the greater increases in condensation with weaker fire intensity. This leads to the greater overall effects of fire-produced aerosols on the UTLS water vapor and ice with weaker fire intensity.

In this section, we see that the smaller R_v leads to lower autoconversion rates and a larger amount of cloud liquid as a source of freezing, which in turn induce higher freezing rates and stronger feedbacks between freezing, deposition, condensation and updrafts in the polluted-scenario run than in the clean-scenario run for each fire intensity. This results in stronger updrafts and their impacts on the UTLS water vapor and ice in the polluted-scenario run than in the clean-scenario run for each fire intensity. The greater R_v reduction among the polluted-scenario runs than among the clean-scenario runs with weakening fire intensity induces the differences in autoconversion, freezing and the feedbacks between the polluted-scenario run and the clean-scenario run to get greater as fire intensity weakens.

Deleted: control run and the low-aerosol run for strong fire intensity, between the medium run and the medium-low run for medium fire intensity, and between the weak run and the weak-low run for weak fire intensity, respectively.

Deleted: Recall that the control run for strong fire intensity, the medium run for medium fire intensity and the weak run for weak fire intensity are the polluted-scenario runs, while the low-aerosol run for strong fire intensity, the medium-low run for medium fire intensity and the weak-low run for weak fire intensity are the clean-scenario runs.

Deleted: over

Deleted: 15

Deleted: 15

Deleted: 6

Deleted: , as seen in

Deleted: 15

Deleted: 6

Deleted: 6

Deleted: 15

Deleted: 6

Deleted: the

Deleted: pyroCb

Formatted: Subscript

Formatted: Subscript

This results in the greater impacts of aerosol-induced stronger updrafts on the UTLS water vapor and ice with weaker fire intensity.

4.3 Dependence of aerosol effects on the magnitude of aerosol perturbation

Table 3 shows that for each of the strong-, medium-, and weak-fire cases, there are increases in the UTLS water-vapor mass and in the amount of the UTLS cirrus clouds in the run with the fire-induced aerosol perturbations of 30000 or 7500 cm^{-3}. These increases are relative to the mass and the amount in the low-aerosol run for the strong-fire case, in the medium-low run for the medium-fire case, and in the weak-low run for the weak-fire case, respectively, with no fire-induced aerosol perturbation. Note that for each of the three types of fire-induced aerosol perturbations of 30000, 15000 and 7500 cm^{-3}, aerosol-perturbation-induced percentage increases in the UTLS water-vapor mass and the amount of UTLS cirrus clouds get greater as fire intensity weakens (Tables 2 and 3). The qualitative nature of results regarding the dependence of the percentage increases in the UTLS water-vapor mass and the amount of the UTLS cirrus clouds on fire intensity thus does not depend on the magnitude of the fire-induced aerosol perturbation.

Until now, we considered the situation where the fire-induced aerosol perturbation does not vary with fire intensity. Note that so far, we have taken interest in the sensitivity to fire intensity of an aerosol perturbation on pyroCb development, the UTLS water vapor, and cirrus clouds. Hence, to examine and isolate the sensitivity, we have shown comparisons among sensitivity simulations by varying only fire intensity while maintaining a constant aerosol perturbation. While working well for the isolation aspect, this strategy does not reflect reality well. It may be that weaker fire intensity produces a smaller aerosol concentration. This possibility is not that unrealistic, since stronger fire likely involves more material burnt and more aerosols from it.

With this situation in mind, we make comparisons among three pairs of simulations: the low-aerosol run and the control-30000 run for strong fire vs. the medium-low run and the medium run for medium fire vs. the weak-low run and the weak-7500 run for weak fire. Hence, among these three pairs, the magnitude of fire-induced aerosol perturbation reduces with weakening fire, emulating the possibility that weaker fire intensity involves a less

Deleted: ¶

Deleted: 2

Deleted: UTLS

Deleted: the

amount of aerosols. For strong fire, the perturbation-related aerosol concentration is 30000 cm^{-3}, for medium fire, it is 15000 cm^{-3}, and for weak fire, it is 7500 cm^{-3}. As shown in Tables 2 and 3, comparisons among these three pairs show that relative importance of aerosol effects on the pyroCb development and its impacts on UTLS water vapor and cirrus clouds increases for weaker fires, and it does not matter if the aerosol perturbation reduces or stays constant with weakening fire intensity. In these comparisons, it is also possible that when fire-induced aerosol perturbation is very low for medium or weak fire intensity, the latent heat perturbation by aerosol perturbation can be very low. This very low latent heat is not large enough to increase the relative importance of those aerosol effects with weakening fire intensity. Based on this, the medium run and the weak run are repeated again. The medium run is repeated with lower fire-induced aerosol perturbations than the perturbation of 15000 cm^{-3}, while the weak run is repeated with lower fire-induced aerosol perturbations than the perturbation of 7500 cm^{-3}. Recall that when the repeated medium run has the aerosol perturbation of 2000 cm^{-3}, the repeated medium run is referred to as the medium-2000 run; when the repeated weak run has the aerosol perturbation of 1000 cm^{-3}, the repeated weak run is referred to as the weak-1000 run. The percentage increases in the UTLS water vapor and cirrus-cloud amount from the medium-low run to the medium-2000 run or from the weak-low run to the weak-1000 run are smaller than those increases, for the case of strong fire, from the low-aerosol run to the control-30000 run. This indicates that when fire-induced aerosol perturbation reduces too much with weakening fire intensity, the relative importance of aerosol effects on pyroCb development and its impacts on the UTLS water vapor and cirrus clouds no longer increases with the weakening fire intensity.

Deleted: the

Results in this section shows that the increasing impacts of fire-induced aerosol perturbations on the UTLS water vapor and cirrus clouds with weakening fire intensity is robust whether those aerosol perturbations vary with varying fire intensity or not, unless the variation of aerosol perturbations is extremely high.

5. Conclusions

Formatted: Font: 14 pt, Bold

Deleted: Summary and c

This study investigates an observed case of a pyroCb using a modeling framework. In particular, this study focuses on effects of fire-produced aerosols on pyroCb development

and its impacts on the UTLS water vapor and cirrus clouds. Results show that pyroCb updrafts transport water vapor to the tropopause and above efficiently. This leads to a much greater amount of water vapor around and above the tropopause (i.e., the UTLS) over the pyroCb as compared to that in the background outside the pyroCb. The pyroCb also generates a deck of cirrus cloud around the tropopause. It is found that the role played by fire-produced aerosols or the fire-induced aerosol perturbation in the water-vapor transportation to UTLS and the production of cirrus cloud in the pyroCb gets more significant as fire intensity weakens.

As fire intensity weakens, due to the reduction in LWC, R_v decreases despite the reduction in CDNC that tends to increase R_v. During the initial stage, there is a similar LWC between the polluted-scenario run (i.e., the control run for strong fire intensity, the medium run for medium fire intensity and the weak run for weak fire intensity with the fire-induced aerosol perturbation) and the clean-scenario run (i.e., the low-aerosol run for strong fire intensity, the medium-low run for medium fire intensity and the weak-low run for weak fire intensity with no fire-induced aerosol perturbation) for each fire intensity. The reduction in LWC with weakening fire intensity among the polluted-scenario runs is also similar to that among the clean-scenario runs. During the initial stage, there are much greater CDNC in the polluted-scenario run than in the clean-scenario run for each fire intensity, and the smaller CDNC reduction among the polluted-scenario runs than among the clean-scenario runs with weakening fire intensity. This situation during the initial stage induces R_v to reduce much more among the polluted-scenario runs than among the clean-scenario runs with weakening fire intensity. This reduces autoconversion more among the polluted-scenario runs than among the clean-scenario runs with weakening fire intensity. This makes differences in autoconversion between the polluted-scenario run and the clean-scenario run increase as fire intensity weakens. The increasing difference in autoconversion between the polluted-scenario run and the clean-scenario run causes greater differences in freezing-related latent heat as fire intensity weakens. Through feedback between freezing, deposition, updrafts, and condensation, differences in freezing-related latent heat induce differences in updrafts between the polluted-scenario run and the clean-scenario run. Those greater differences in freezing-related latent heat also lead to greater differences in updrafts, producing the greater differences in the UTLS water vapor and cirrus clouds between the

Deleted: (i.e., the control run, the medium run and the weak run)

Deleted: (i.e., the low-aerosol run, the medium-low run and the weak-low run)

Deleted: enhance

Deleted: enhancing

runs with weaker fire intensity. This means that the role of fire-produced aerosols in water-vapor transport to the UTLS and the production of cirrus cloud in the pyroCb becomes more significant as fire intensity weakens.

The more significant role of fire-produced aerosols in water-vapor transport to the UTLS and the production of cirrus cloud in the pyroCb with weaker fire intensity is robust to the magnitude of the given fire-induced aerosol perturbation which was assumed not to vary with varying fire intensity. This more significant role with weaker fire intensity is also robust to the variation of the fire-induced aerosol perturbation with the varying fire intensity unless the variation is very high.

It is true that the level of the understanding of a mechanism that controls the role played by fire-produced aerosols in the development of pyroCbs and their impacts on the UTLS water vapor and cirrus clouds has been low. This study shows that fire-produced aerosols can invigorate convection and updrafts and thus cause enhanced transportation of water vapor to the UTLS and enhanced formation of cirrus clouds. This study finds that the mechanism that controls the invigoration of convection by aerosols in the pyroCb is consistent with the traditional invigoration mechanism which was proposed and detailed in Rosenfeld et al. (2008). However, this study shows that for pyroCbs produced by strong fires, the aerosol-induced invigoration and its effects on the UTLS water vapor and cirrus clouds are insignificant. Note that traditional understanding generally focuses on effects of fire-produced heat and water vapor and their associated fluxes around the surface on the pyroCb and does not consider effects of fire-produced aerosols on the pyroCb, and this understanding adequately explains the mechanics for pyroCbs in association with strong fires. However, this study suggests that the role of fire-produced aerosols in pyroCb development and its effects on the UTLS water vapor and cirrus clouds should be considered for cases where pyroCbs form over weak-intensity fires, should one be observed in nature.

It is of interest to note that when fire-induced aerosol perturbations are strongly reduced for cases of weaker-intensity fires compared with strong-intensity fires, the significance of the role played by fire-produced aerosol perturbation does not increase any longer and starts to reduce with weakening fire. This suggests that there is a critical level

Deleted: is

Deleted:

Deleted: which is more significant

Deleted: in the UTLS

Deleted: in the UTLS

of aerosol perturbation below which the increase in the significance with weakening fire intensity ceases.

Author contributions

SSL came up with the research goals and aims, preformed the simulations, and wrote the manuscript. GK and ZL selected the case, analyzed observations, and provided data to set up the simulations while reviewing and providing comments on the manuscript. CHJ and YSC revised manuscript based on the reviewers' comments and perform associated analyses of simulation and observation data.

Acknowledgements

This study is supported by the National Aeronautics and Space Administration through grant NNX16AN61G and the National Science Foundation through grant AGS 1837811. This study was also supported by the National Strategic Project-Fine particle of the National Research Foundation of Korea (NRF) funded by the Ministry of Science and ICT (MSIT), the Ministry of Environment (ME), the Ministry of Health and Welfare (MOHW) (NRF-2017M3D8A1092022) and the ministry of Education (NRF-2018R1D1A1A09083227).

Deleted: (NASA)

Deleted: supported

Formatted: Font: (Asian) Malgun Gothic, Font color: Black

Formatted: Font: (Default) Times New Roman, (Asian) Malgun Gothic, 12 pt, Font color: Black, Pattern: Clear

Formatted: Font: (Asian) Malgun Gothic, Font color: Black

Deleted: ¶

References

Albrecht, B. A.: Aerosols, cloud microphysics, and fractional cloudiness, Science, 245, 1227-1230, 1989.

Andreae, M. O., Rosenfeld, D., Artaxo, P., Costa, A. A., Frank, G. P., Longo, K. M., and Silva-Dias, M. A. F.: Smoking rain clouds over the Amazon, Science, 303, 1337–1342, 2004.

Fan, J., Leung, L. R., Li, Z.: Aerosol impacts on clouds and precipitation in eastern China: Results from bin and bulk microphysics, J. Geophys. Res., 117, D00K36, doi:10.1029/2011JD016537, 2012.

Fouquart, Y., and Bonnel, B.: Computation of solar heating of the Earth's atmosphere: a new parameterization, Beitr. Phys. Atmos., 53, 35-62, 1980.

Fromm, M., Lindsey, D. T., Servranckx, R., Yue, G., Trickl, T., Sica, R., Doucet, P., Godin-Beekmann, S., et al.: The untold story of pyrocumulonimbus, B. Am. Meteorol. Soc., 91, 1193, doi:10.1175/2010BAMS3004.1, 2010.

Grabowski, W. W., Wu, X., Moncrieff, M. W.: Cloud resolving modeling of tropical cloud systems during phase III of GATE. Part I: Two-Dimensional Experiments, J. Atmos. Sci., 53, 3684-3709, 1996.

Houze, R. A.: Cloud dynamics, Academic Press, 573 pp, 1993.

Kablick, G., Fromm, M., Miller, S., Partain, P., Peterson. D., Lee, S. S., Zhang, Y., Lambert, A., and Li, Z.: The Great Slave Lake pyroCb of 5 August 2014: observations, simulations, comparisons with regular convection, and impact on UTLS water vapor, J. Geophy. Res., https://doi.org/10.1029/2018JD028965, 2018.

Emanuel, K.: Atmospheric convection, Oxford University Press, 580 pp, 1994.

Khain, A., Ovtchinnikov, M., Pinsky, M.: Notes on the state-of-the-art numerical modeling of cloud microphysics, Atmos. Res., 55, 159-224, 2000.

Khain, A.: Notes on state-of-the-art investigations of aerosol effects on precipitation: a critical review, Environ. Res. Lett., 4, doi:10.1088/1748-9326/4/1/015004, 2009.

Khain, A., BenMoshe, N., and Pokrovsky, A.: Factors determining the impact of aerosols on surface precipitation from clouds: Attempt of classification, J. Atmos. Sci., 65, 1721-1748, 2008.

Formatted: Font: (Asian) Malgun Gothic, Font color: Black

Formatted: Font: (Asian) Malgun Gothic, Font color: Black

Formatted: Font: (Asian) Malgun Gothic, Not Italic, Font color: Black

Formatted: Font: (Asian) Malgun Gothic, Font color: Black

Formatted: Font: (Asian) Malgun Gothic, 12 pt, Font color: Black

Formatted: Indent: Left: 0", Hanging: 2 ch

Formatted: Font: (Asian) Malgun Gothic, 12 pt, Font color: Black

Formatted: Font: (Asian) Malgun Gothic, 12 pt, Font color: Black

Formatted: Font: (Asian) Malgun Gothic, 12 pt, Font color: Black

Formatted: Font: (Asian) Malgun Gothic, 12 pt, Font color: Black

Formatted: Font: (Asian) Malgun Gothic, Font color: Black

Formatted: Font: (Asian) Malgun Gothic, Font color: Black

Formatted: Font: (Asian) Malgun Gothic, Font color: Black

Formatted: Font: (Asian) Malgun Gothic, Font color: Black

Formatted: Font: (Asian) Malgun Gothic, Not Italic, Font color: Black

Formatted: Font: (Asian) Malgun Gothic, Font color: Black

Khain, A. P., et al.: Representation of microphysical processes in cloud resolving models: Spectral (bin) microphysics versus bulk parameterization, Rev. Geophys., 53, 247–322, doi:10.1002/2014RG000468, 2015.

Khairoutdinov, M., and Kogan, Y.: A new cloud physics parameterization in a large-eddy simulation model of marine stratocumulus, Mon. Wea. Rev., 128, 229-243, 2000.

Knobelspiesse, K., Cairus, B., Ottaviani, M., et al.: Combined retrievals of boreal forest fire aerosol properties with a polarimeter and lidar, Atmos. Chem. Phys., 11, 7045-7067, 2011.

Koop, T., Luo, B. P, Tsias, A. and Peter, T,: Water activity as the determinant for homogeneous ice nucleation in aqueous solutions, Nature, 406, 611-614. 2000.

Koren, I., Altaratz, O., Remer, L. A., et al.: Aerosol-induced intensification of rain from the tropics to the mid-latitudes, Nat. Geosci., 5, 118-122, 2012.

Krueger, S. K., Cederwall, R. T., Xie, S. C., and Yio, J. J.: GCSS Working Group 4 Model Intercomparison-procedures for Case 3: Summer 1997 ARM SCM IOP. Draft manuscript obtainable from http://www.arm.gov/docs/scm/scmic3, 1999.

Lebo, Z. J. and Morrison, H.: Effects of horizontal and vertical grid spacing on mixing in simulated squall lines and implications for convective strength and structure, Mon. Wea. Rev., 143, 4355-4375, 2014.

Lee, H., and Baik, J.-J.: A physically based autoconversion parameterization, J. Atmos. Sci., 74, 1599-1615, 2017.

Lee, S. S., Donner, L. J., Phillips, V. T. J., and Ming, Y.: The dependence of aerosol effects on clouds and precipitation on cloud-system organization, shear and stability, J. Geophys. Res., 113, D16202, 2008.

Lee, S. S., Feingold, G., Koren, I., Yu, H., Yamaguchi, T., and McComiskey, A.: Effect of gradients in biomass burning aerosol on circulations and clouds, J. Geophys. Res., 119, 9948-9964, 2014.

Lee, S. S., Kim, B. -G., Yum, S. S., et al.: Effect of aerosol on evaporation, freezing and precipitation in a multiple cloud system, Clim. Dyn., 48, 1069-1087, 2016.

Lee, S. S., Li, Z., and Mok, J., et al.: Interactions between aerosol absorption, thermodynamics, dynamics, and microphysics and their impacts on clouds and precipitation in a multiple-cloud system, Clim. Dyn., 49, 3905-3921, 2017.

Formatted: Font: (Asian) Malgun Gothic, Font color: Black

Formatted: Font: (Asian) Malgun Gothic, Font color: Black

Formatted: Font: (Asian) Malgun Gothic, Font color: Black

Formatted: Font: (Asian) Malgun Gothic, Font color: Black

Formatted: Font: (Asian) Malgun Gothic, Font color: Black

Formatted: Font: (Asian) Malgun Gothic, Font color: Black

Formatted: Font: (Asian) Malgun Gothic, Font color: Black

Formatted: Font: (Default) Times New Roman, (Asian) Malgun Gothic, 12 pt

Formatted: Font: (Default) Times New Roman, (Asian) Malgun Gothic, 12 pt

Formatted: Font: (Default) Times New Roman, (Asian) Malgun Gothic, 12 pt

Formatted: Font: (Default) Times New Roman, (Asian) Malgun Gothic, 12 pt

Formatted: Font: (Default) Times New Roman, (Asian) Malgun Gothic, 12 pt

Formatted: Font: (Default) Times New Roman, (Asian) Malgun Gothic, 12 pt

Formatted: Font: (Default) Times New Roman, (Asian) Malgun Gothic, 12 pt

Formatted: Font: (Default) Times New Roman, (Asian) Malgun Gothic, 12 pt

Formatted: Font: (Default) Times New Roman, (Asian) Malgun Gothic, 12 pt

Formatted: Font: (Default) Times New Roman, (Asian) Malgun Gothic, 12 pt

Formatted: Font: (Default) Times New Roman, (Asian) Malgun Gothic, 12 pt

Formatted: Font: (Default) Times New Roman, (Asian) Malgun Gothic, 12 pt

Formatted: Font: (Default) Times New Roman, (Asian) Malgun Gothic, 12 pt

1833 Lee, S. S., and Penner, J. E.: Comparison of a global-climate model to a cloud-system
1834 resolving model for the long-term response of thin stratocumulus clouds to
1835 preindustrial and present-day aerosol conditions, Atmos. Chem. Phys., 10, 6371-6389,
1836 2010.
1837 Lee, S. S., Penner, J. E., and Saleeby, S. M.: Aerosol effects on liquid-water path of thin
1838 stratocumulus clouds., J. Geophys. Res., 114, D07204, 2009.
1839 Liu, Y., and Daum, P. H.: Parameterization of the autoconversion process. Part I: Analytical
1840 formulation of the Kessler-type parameterizations, J. Atmos. Sci., 61, 1539-1548,
1841 2004.
1842 Lohmann, U. and Diehl, K.: Sensitivity studies of the importance of dust ice nuclei for the
1843 indirect aerosol effect on stratiform mixed-phase clouds, J. Atmos. Sci., 63, 968-982,
1844 2006.
1845 Luderer, G., Trentmann, J., Winterrath, T., Textor, C., Herzog, M., Graf, H., and Andreae,
1846 M.: Modeling of biomass smoke injection into the lower stratosphere by a large forest
1847 fire (part ii): Sensitivity studies. Atmos. Chem. Phy., 6, 5261–5277, 2006.
1848 Luderer, G., Trentmann, J., and Andreae, M.: A new look at the role of fire-released
1849 moisture on the dynamics of atmospheric pyro-convection, Int. J. Wildland Fire, 18,
1850 554-562, 2009.
1851 Mlawer, E. J., Taubman, S. J., Brown, P. D., Iacono, M. J., and Clough, S. A.: RRTM, a
1852 validated correlated-k model for the longwave, J. Geophys. Res., 102, 16663-1668,
1853 1997.
1854 Möhler, O., et al.: Efficiency of the deposition mode ice nucleation on mineral dust particles,
1855 Atmos. Chem. Phys., 6, 3007-3021, 2006.
1856 Morrison, H., and Grabowski, W. W.: Cloud-system resolving model simulations of aerosol
1857 indirect effects on tropical deep convection and its thermodynamic environment,
1858 Atmos. Chem. Phys., 11, 10503-10523, 2011.
1859 Peterson, D., Fromm, M., Solbrig, J., Hyer, E., Surratt, M., and Campbell, J.: Detection
1860 and inventory of intense pyroconvection in western North America using GOES-15
1861 daytime infrared data, J. Appl. Meteorol. Clim., 56, 471-493, 2017.
1862 Phillips, V. T. J., Donner, L. J., and Garner, S.: Nucleation processes in deep convection
1863 simulated by a cloud-system-resolving model with double-moment bulk microphysics,

Deleted: ¶
Formatted: Font color: Black
Formatted: Font: Not Bold
Formatted: Font: Not Bold
Formatted: Font: Not Bold
Formatted: Font: Not Bold
Formatted: Font: (Asian) Malgun Gothic, 12 pt, Font color: Black, (Asian) Korean
Formatted: Font: (Asian) Malgun Gothic, 12 pt, Font color: Black, (Asian) Korean
Formatted: Font: (Asian) Malgun Gothic, Font color: Black
Formatted: Font: (Asian) Malgun Gothic, Font color: Black
Formatted: Font: (Asian) Malgun Gothic, Font color: Black

J. Atrmos. Sci., 64, 738-761, 2007.

Pruppacher, H. R., and Klett, J. D.: Microphysics of clouds and precipitation, 714pp, Reidel D., 1978.

Pumphrey, H., Santee, M., Livesey, N., Schwartz, M., and Read, W.: Microwave Limb Sounder observations of biomass-burning products from the Australian bush fires of February 2009, Atmos. Chem. Phys., 11, 6285-6296, 2011.

Reid, J. S., Hobbs, P. V., Rangno, A. L., and Hegg, D. A.: Relationships between cloud droplet effective radius, liquid water content, and droplet concentration for warm clouds in Brazil embedded in biomass smoke, J. Geophys. Res., 104, 6145-6153, 1999.

Reid, J. S., Koppmann, R., Eck T. F., and Eleuterio, D.: A review of biomass burning emissions part II: intensive physical properties of biomass burning particles, Atmos. Chem. Phys., 5,799-825, 2005.

Rogers, R. R., and Yau, M. K.: A short course in cloud physics, Pergamon Press, 293pp, 1991.

Rosenfeld, D., Lohmann, U., Raga, G. B., et al.: Flood or drought, How do aerosols affect precipitation? Science, 321, 1309-1313, 2008.

Seinfeld, J. H. and Pandis, S. N.: Atmospheric Chemistry and Physics: From Air Pollution to Climate Change, John Wiley & Sons, 1326 pp, 1998.

Solomon, S., Rosenlof, K. H., Portmann, R. W., Daniel, J. S., Davis, S. M., Sanford, T. J., and Plattner, G. K.: Contributions of stratospheric water vapor to decadal changes in the rate of global warming, Science, 327, 1219–1223, 2010.

Storer, R. L., van den Heever, S. C., and Stephens, G. L.: Modeling aerosol impacts on convection under differing storm environments, J. Atmos. Sci., 67, 3904-3915, 2010.

Tao, W.-K., Chen, J.-P., Li, Z., Wang, C., and Zhang, C.: Impact of aerosols on convective clouds and precipitation, Rev. Geophys., 50, RG2001, 2012.

Trentmann, J., Luderer, G., Winterrath, T., Fromm, M., Servranckx, R., Textor, C., et al.: Modeling of biomass smoke injection into the lower stratosphere by a large forest fire (part i): reference simulation. Atmos. Chem. Phys., 6, 5247–5260, 2006.

Twomey, S.: The influence of pollution on the shortwave albedo of clouds, J. Atmos. Sci., 34, 1149-1152, 1977.

Wang, H., Skamarock, W. C., and Feingold, G.: Evaluation of scalar advection schemes in

Formatted: Font: (Default) Times New Roman, (Asian) Malgun Gothic, Not Italic, Font color: Black

Formatted: Font: (Default) Times New Roman, (Asian) Malgun Gothic, Font color: Black

Formatted: Font: (Default) Times New Roman, (Asian) Malgun Gothic, Not Italic, Font color: Black

Deleted:

Formatted: Font: (Asian) Malgun Gothic, 12 pt, Font color: Black

Formatted: Indent: Left: 0", Hanging: 2 ch

Formatted: Font: (Asian) Malgun Gothic, 12 pt, Font color: Black

Deleted: .

Formatted: Font: (Asian) Malgun Gothic, Font color: Black

Formatted: Font: (Asian) Malgun Gothic, Font color: Black

Formatted: Font: (Asian) Malgun Gothic, Not Italic, Font color: Black

Formatted: Font: (Asian) Malgun Gothic, Font color: Black

the Advanced Research WRF model using large-eddy simulations of aerosol-cloud interactions, Mon. Wea. Rev., 137, 2547-2558, 2009.

FIGURE CAPTIONS

Figure 1. VIIRS visible image of the fire, smoke and cirrus cloud which are associated with the selected pyroCb. Bright white represents cirrus (anvil) at the top of the pyroCb, while the red circle marks the fire spot. Dark white represents smoke produced by the fire. Adapted from Kablick et al. (2018).

Figure 2. The simulated fire spot (red circle) and the field of cloud-ice mass density (cirrus cloud) at the top of the simulated pyroCb when the pyroCb is about to advance to its mature stage.

Figure 3. The vertical distribution of the radar reflectivity which is averaged over the Cloudsat path.

Figure 4. Vertical distributions of the averaged updraft mass fluxes at all altitudes in cloudy areas (where the sum of LWC and IWC is non-zero) over the simulation period between 17:00 GMT on August 5th and 12:00 GMT on August 6th.

Figure 5. Vertical distributions of average water-vapor mass density at altitudes above 13 km and over the simulation period between 17:00 GMT on August 5th and 12:00 GMT on August 6th. Colored lines represent the averaged values over cloudy grid columns (non-zero sum of LWP and IWP). The black line represents those values over non-cloudy columns (zero sum of LWP and IWP) in the control run.

Figure 6. Vertical distributions of the averaged cloud-ice mass density at all altitudes in cloudy areas (non-zero sum of LWC and IWC) over the simulation period between 17:00 GMT on August 5th and 12:00 GMT on August 6th.

Figure 7. Same as Figure 6 but for deposition rate.

Deleted: Figure 1. VIIRS visible image of fire, smoke and cirrus cloud which are associated with the selected pyroCb. The bright white represents cirrus cloud or anvil cloud at the top of the pyroCb, while the red circle marks the fire spot. The dark white represents smoke produced by fire. Adapted from Kablick et al. (2018).¶

Deleted: The red circle marks the simulated fire spot, while the field represents the simulated cirrus cloud.

Deleted: Figure 3. Initial aerosol size distribution in the PBL over the fire spot. N represents aerosol number concentration per unit ... [17]

Deleted: 4

Deleted: 5

Deleted: over

Deleted: areas,

Deleted: liquid-water content (

Deleted:)

Deleted: ice-water content (

Deleted:)

Deleted: ,

Deleted: and

Deleted: in the control run and the low-aerosol run

Deleted: 6

Formatted: Superscript

Formatted: Superscript

Deleted: Vertical distributions of the averaged water-vapor mass ... [18]

Deleted: Colored

Deleted: over

Deleted: where there is the

Deleted: liquid-water path (

Deleted:)

Deleted: ice-water path (

Deleted:)

Deleted: in the control run and the low-aerosol run,

Deleted: while t

Deleted: where there is the

Deleted: 7

Deleted: over

Deleted: , where the

Deleted: liquid-water content (

Deleted:)

Deleted: ice-water content (

Deleted:)

Deleted: is non-zero, and

Deleted: in the control run and the low-aerosol run

Deleted: 8

Deleted: Vertical distributions of the averaged deposition rate over ... [19]

Deleted: ¶ ... [20]

Figure 8. The averaged CDNC, R_v, and LWC at all altitudes in cloudy areas, over the period between 17:00 and 19:00 GMT on August 5th.

Figure 9. The averaged rates of condensation, deposition and cloud-liquid freezing at all altitudes in cloudy areas and over periods (a) 2, (b) 3 and (c) 4. In panel (a), the average autoconversion rates are additionally shown.

Figure 10. Time series of differences in the average values of variables related to aerosol-induced invigoration of convection, at all altitudes in cloudy areas between the (a) control and low-aerosol runs for strong fire intensity, (b) medium and medium-low runs for medium fire intensity and (c) weak and weak-low runs for weak fire intensity.

Deleted: 12

Deleted: over

Deleted: at all altitudes and

Deleted: ¶

Deleted: Figure 13. Graphic depiction of y values as a function of "$x^{\frac{1}{3}}$". x_{L1} and x_{L2} represent large x values, while x_{S1} and x_{S2} represent small x values. y values corresponding to x_{L1}, x_{L2}, x_{S1} and x_{S2} are y_{L1}, y_{L2}, y_{S1} and y_{S2}, respectively. The variation of x value from x_{L1} to x_{L2} is greater than that from x_{S1} to x_{S2}.¶

¶

Figure 14. Diagrammatic depiction of the varying minimum size of aerosol activation with varying fire intensity in the unimodal aerosol size distribution which is assumed in this study. The details of the varying minimum size are described in Section 4.1.2. D_{cs} and D_{cw} represent the minimum size in the low-aerosol run for strong fire intensity and in the weak-low run for weak fire intensity, respectively, while D_{ps} and D_{pw} represent the minimum size in the control run for strong fire intensity and in the weak run for weak fire intensity, respectively. Here, the variation of the minimum size from D_{cs} to D_{cw} is identical to that from D_{ps} to D_{pw}. ¶

Deleted: 15

Deleted: over

Deleted: at all altitudes

Deleted: periods

Deleted: period

Deleted: period

Deleted: d

Deleted: over cloudy areas at all altitudes and over periods 2

Deleted: is

Deleted: 6

Deleted: Time series of differences in the averaged values of variables, which are related to aerosol-induced invigoration of convection, over cloudy areas at all altitudes (a) between the control run and the low-aerosol run for strong fire intensity, (b) between the medium run and the medium-low run for medium fire intensity and (c) between the weak run and the weak-low run for weak fire intensity. …

Deleted: ¶

Simulations	Surface sensible heat fluxes in the fire spot (W m^{-2})	Surface latent heat fluxes in the fire spot (W m^{-2})	Aerosol concentration in the PBL over the fire spot (cm^{-3})
Control run	15000	1800	15000
Low-aerosol run	15000	1800	150
Control-30000	15000	1800	30000
Control-7500	15000	1800	7500
Medium run	7500	900	15000
Medium-low run	7500	900	150
Medium-30000	7500	900	30000
Medium-7500	7500	900	7500
Medium-2000	7500	900	2000
Weak run	3750	450	15000
Weak-low run	3750	450	150
Weak-30000	3750	450	30000
Weak-7500	3750	450	7500
Weak-1000	3750	450	1000

Table 1. Summary of simulations

Deleted:

Deleted: ¶

	Backg-round	Control	Low-aerosol	Differe-nce (%)	Medium	Meidum-low	Differe-nce (%)	Weak	Weak-low	Differe-nce (%)
Updraft mass fluxes (kg m^{-2} s^{-1})		1.23	1.19	3	0.89	0.70	27	0.42	0.21	100
Water-vapor mass density between 13 and 16 km (10^{-3} g m^{-3})	0.46	2.31	2.26	2	1.61	1.32	22	0.93	0.58	60
Cirrus-cloud mass density between 9 and 13 km (g m^{-3})		0.024	0.023	4	0.017	0.012	42	0.008	0.004	100

Table 2. The averaged updraft mass fluxes at all altitudes in cloudy areas, the averaged water-vapor mass density over altitudes between 13 and 16 km and over cloudy columns except for the averaged background water-vapor mass density which is also over altitudes between 13 and 16 km but over non-cloudy columns, and the averaged cirrus-cloud mass density between 9 and 13 km in cloudy areas. 16 km is an altitude to which the non-zero water-vapor mass density over cloudy columns extends (Figure 5). These averaged values are obtained over the simulation period between 17:00 GMT on August 5th and 12:00 GMT on August 6th. "Difference" is the percentage difference between the polluted-scenario run and the clean-scenario run for each fire intensity ($\frac{The\ polluted-scenario\ run\ minus\ the\ clean-scenario\ run}{The\ clean-scenario\ run} \times 100$ (%)).

Deleted: over

Deleted: at all altitudes

Deleted: over

Deleted: between 9 and 13 km

Deleted: .

Deleted: Note that the control run for strong fire intensity, the medium run for medium fire intensity and the weak run for weak fire intensity constitute the polluted-scenario runs with higher aerosol concentrations over the fire spot, and the low-aerosol run for strong fire intensity, the medium-low run for medium fire intensity and the weak-low run for weak fire intensity constitute the clean-scenario runs with lower aerosol concentrations over the fire spot. The percentage difference is

	Control-30000	Control-7500	Medium-30000	Medium-7500	Medium-2000	Weak-30000	Weak-7500	Weak-1000
Water vapor mass density between 13 and 16 km (10^{-3} g m^{-3})	2.38 (5%)	2.28 (0.9%)	1.87 (42%)	1.50 (14%)	1.36 (3%)	1.31 (125%)	0.75 (29%)	0.60 (3%)
Cirrus cloud mass density between 9 and 13 km (g m^{-3})	0.025 (9%)	0.023 (0.2%)	0.023 (92%)	0.014 (17%)	0.012 (3%)	0.013 (225%)	0.006 (50%)	0.004 (8%)

Table 3. The averaged water-vapor mass density between 13 and 16 km over cloudy columns and, the averaged cirrus-cloud mass density between 9 and 13 km in cloudy areas over the simulation period between 17:00 GMT on August 5th and 12:00 GMT on August 6th. The numbers in parentheses are the percentage differences: $\frac{The\ control-30000\ (or\ the\ control-7500)\ run\ minus\ the\ low-aerosol\ run}{The\ low-aerosol\ run} \times 100\ (\%)$ for strong fire intensity, $\frac{The\ medium-30000\ (or\ the\ medium-7500\ or\ the\ medium-2000)\ run\ minus\ the\ medium-low\ run}{The\ medium-low\ run} \times 100\ (\%)$ for medium fire intensity, and $\frac{The\ weak-30000\ (or\ the\ weak-7500\ or\ the\ weak-1000)\ run\ minus\ the\ weak-low\ run}{The\ weak-low\ run} \times 100\ (\%)$ for weak fire intensity.

Deleted: between 13 and 16 km
Deleted: over
Deleted: between 9 and 13 km
Deleted: . These averaged values are obtained
Deleted: i
Deleted: is
Deleted: which is

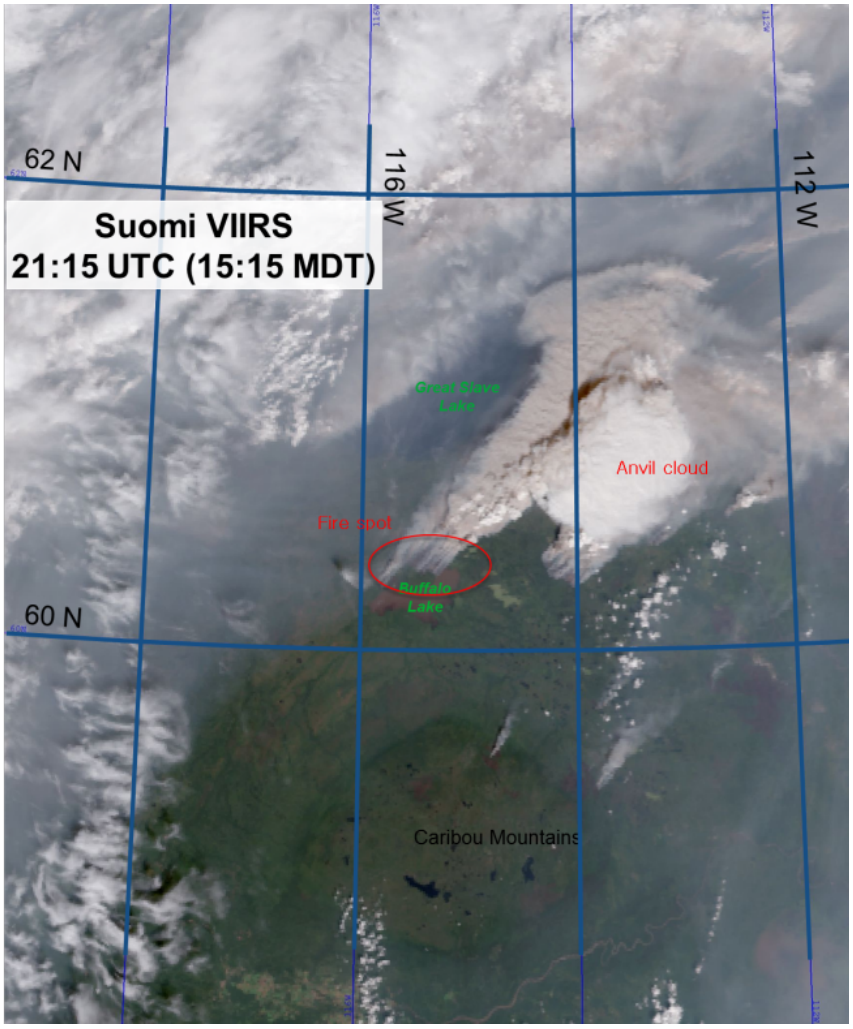
62 N
116 W
112 W
Suomi VIIRS
21:15 UTC (15:15 MDT)
Great Slave Lake
Anvil cloud
Fire spot
Buffalo Lake
60 N
Caribou Mountains

Figure 1

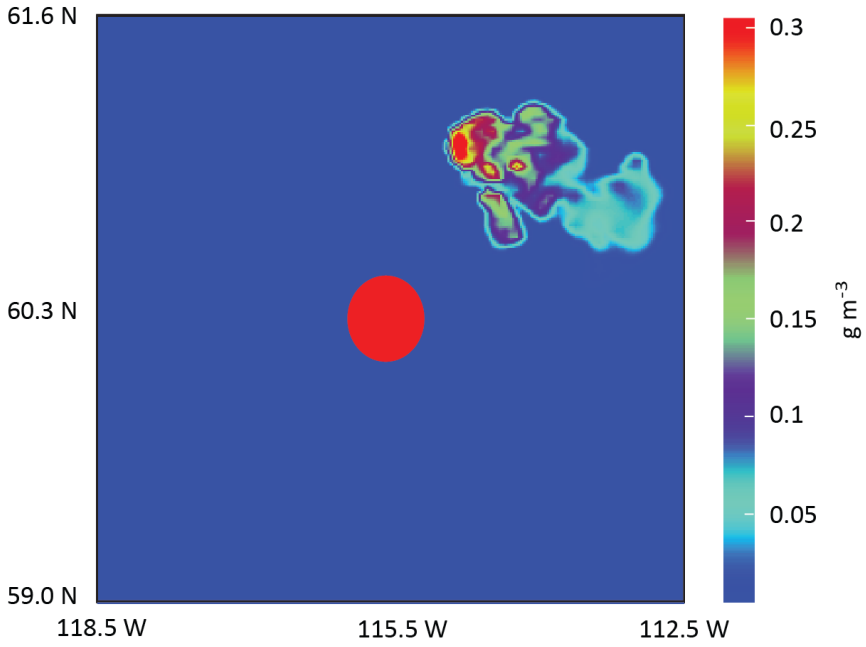

Figure 2

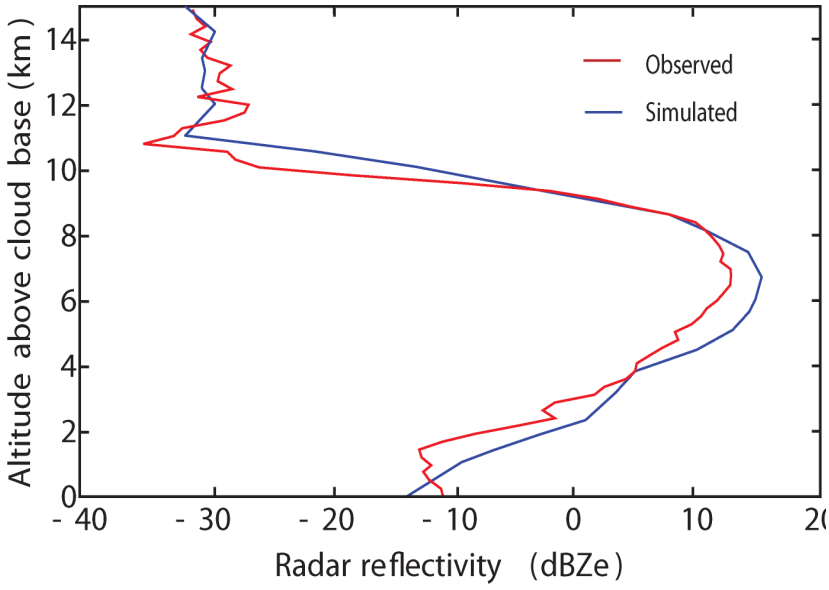

Figure 3

Deleted: ¶

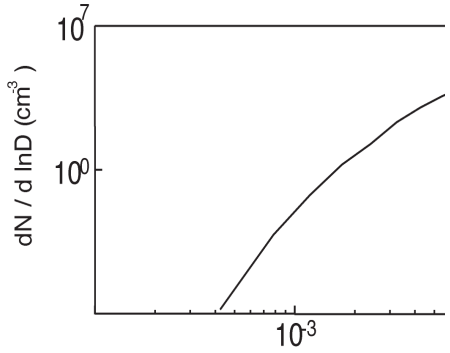

Figure 3¶

Deleted: 4

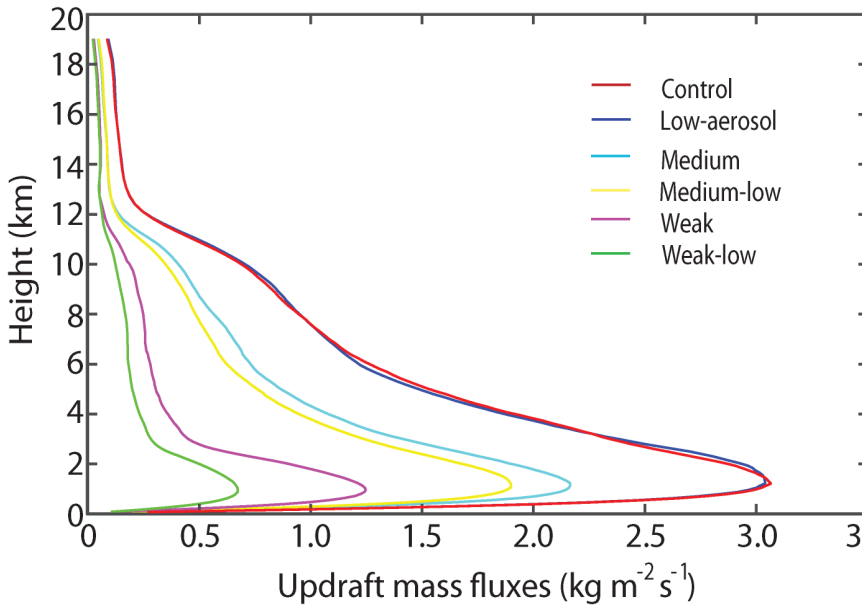

Figure 4

Deleted:

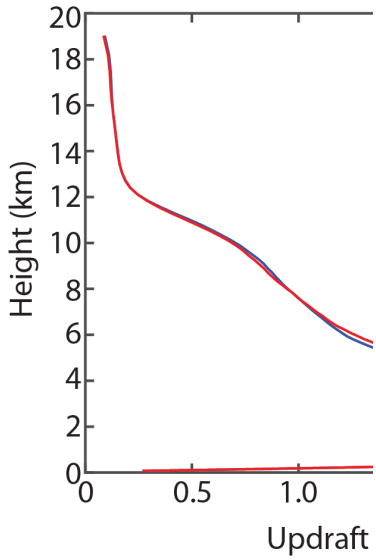

Figure 5¶

... [21]

Deleted: 9

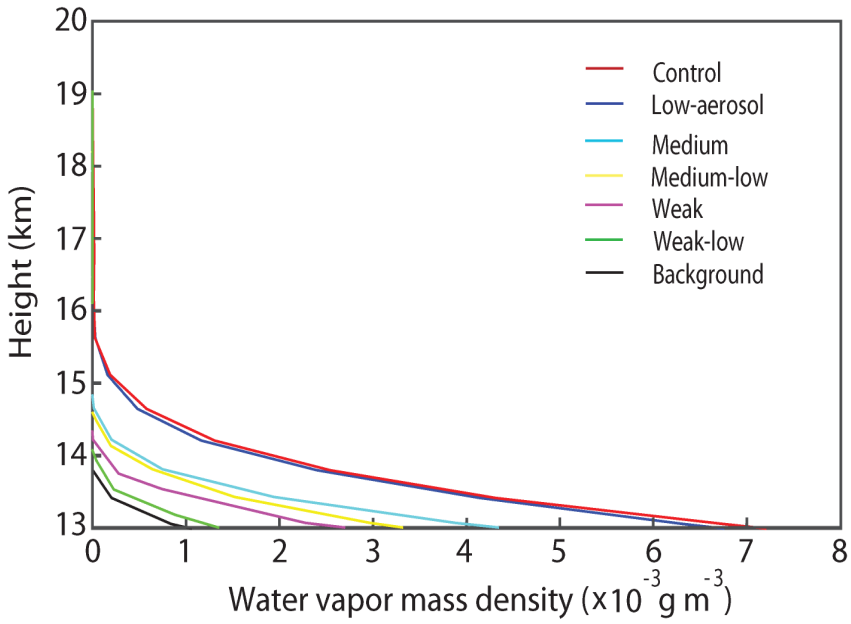

Figure 5

Deleted: 10

Deleted: ¶

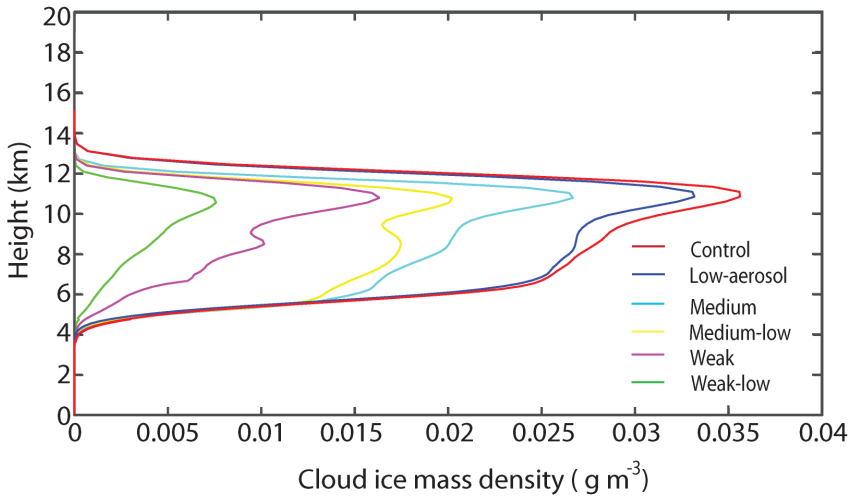

Figure 6

Deleted: 11

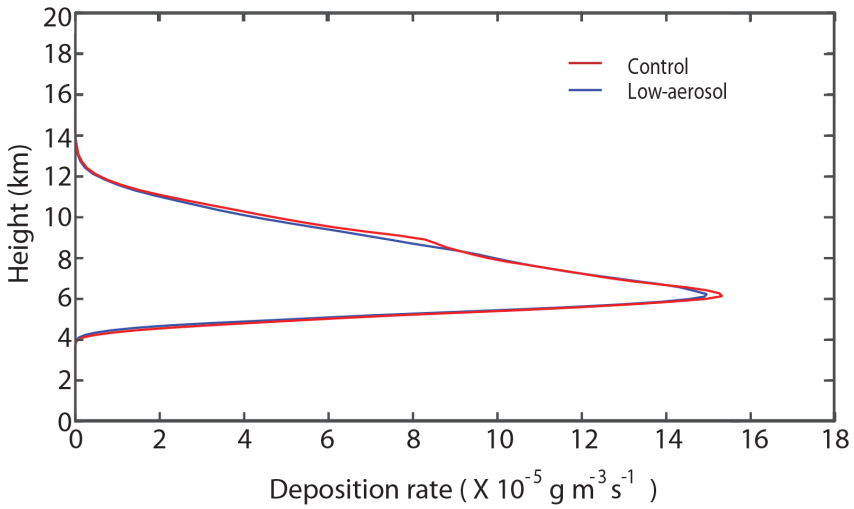
Control
Low-aerosol
Height (km)
Deposition rate (X 10-5 g m-3 s-1)
0
2
4
6
8
10
12
14
16
18
20

Figure 7

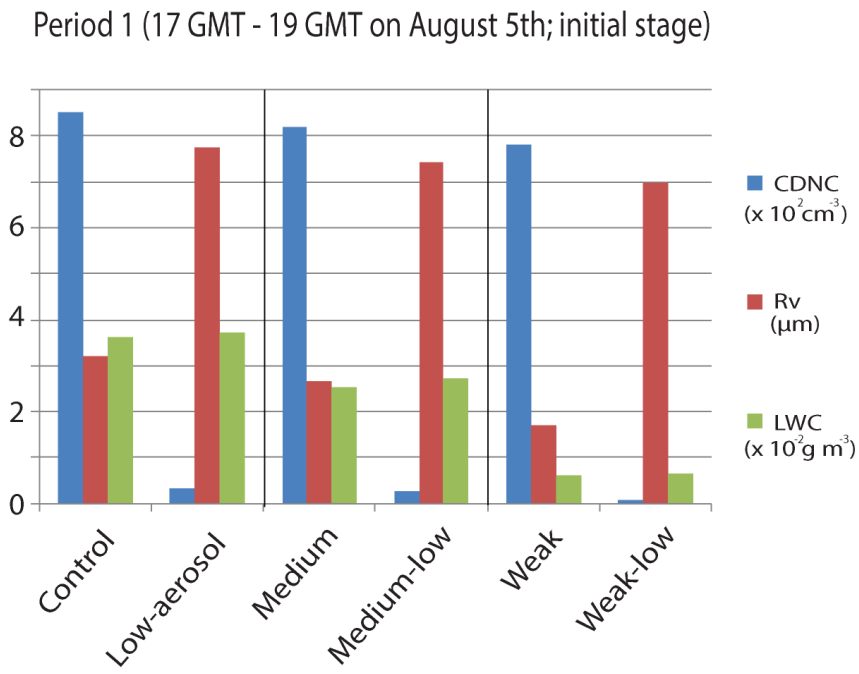

Figure 8

Deleted: 12

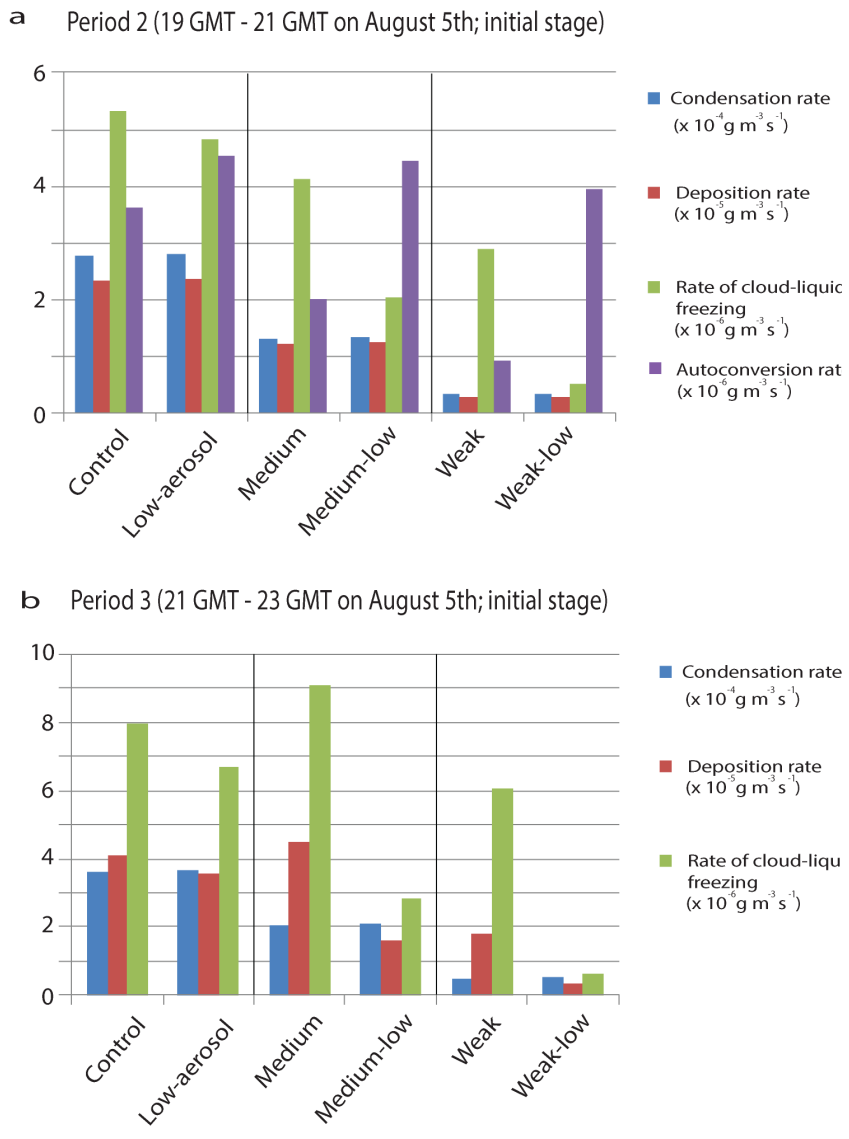

Figure 9

Deleted: ¶

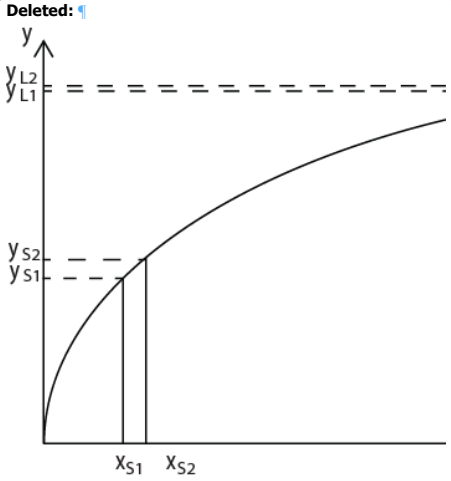

Figure 13¶

¶
¶
¶
¶
¶
¶

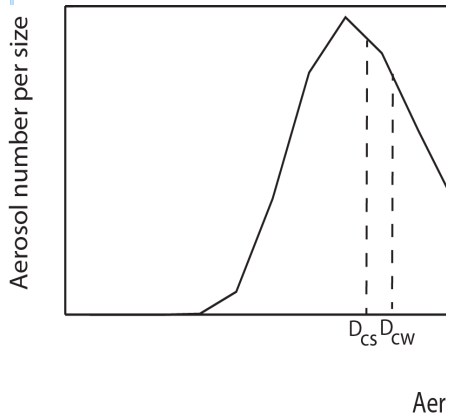

Figure 14¶

¶
¶
¶
¶
¶
¶
¶
¶
¶

Deleted: 15

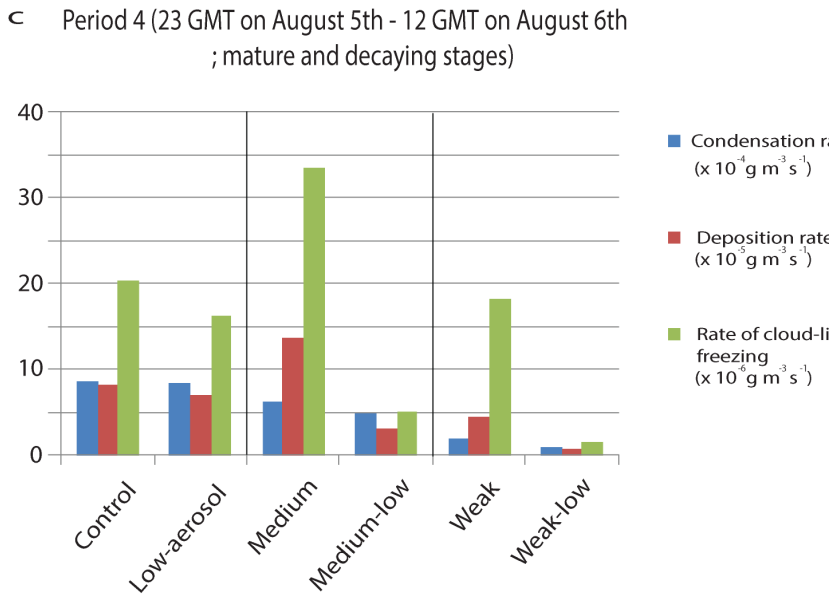

Figure 9

Deleted: 15

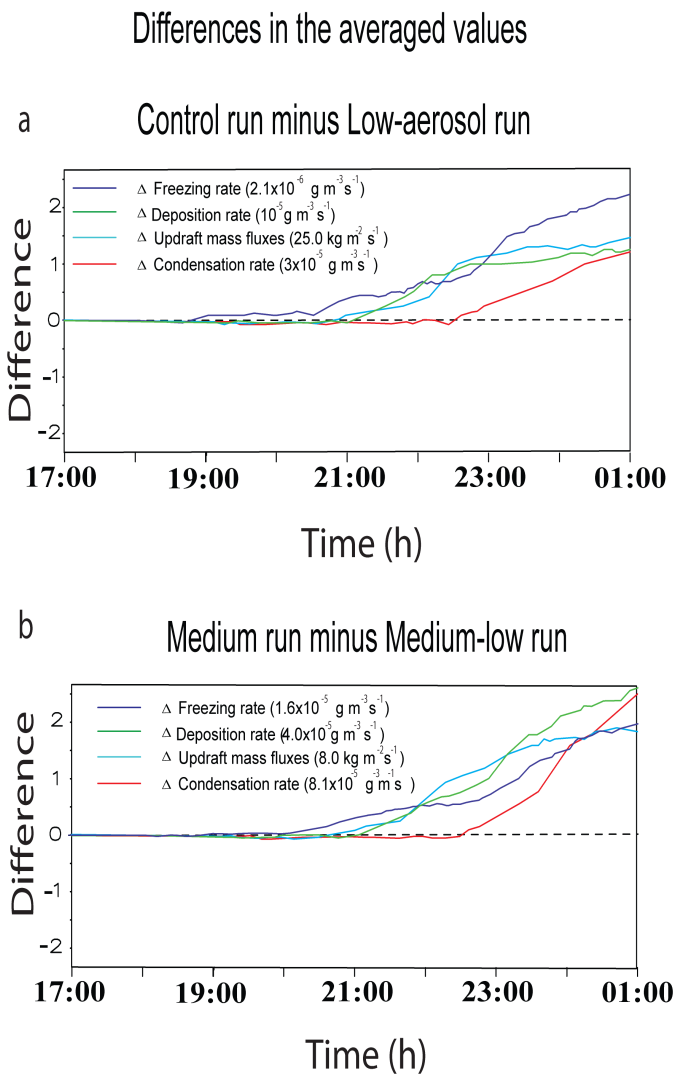

2325

2326 **Figure 10**

Deleted: 6

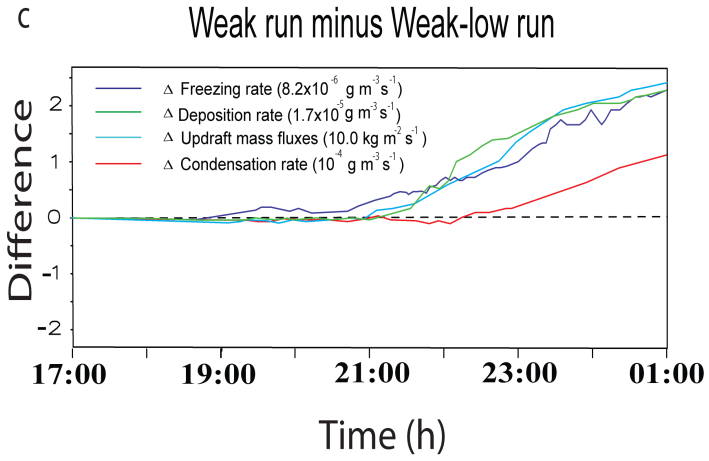

Figure 10

Deleted: 6

Page 43: [1] Deleted	**Seoung Soo Lee**	**8/26/19 7:08:00 AM**
Page 43: [2] Deleted	**Seoung Soo Lee**	**8/26/19 7:15:00 AM**
Page 43: [3] Deleted	**Seoung Soo Lee**	**8/3/19 8:08:00 AM**
Page 43: [4] Deleted	**Seoung Soo Lee**	**8/27/19 7:14:00 AM**
Page 43: [5] Deleted	**Seoung Soo Lee**	**8/27/19 7:29:00 AM**
Page 43: [6] Deleted	**Seoung Soo Lee**	**8/28/19 7:17:00 AM**
Page 43: [7] Deleted	**Seoung Soo Lee**	**8/28/19 7:18:00 AM**
Page 43: [8] Deleted	**Seoung Soo Lee**	**8/27/19 7:31:00 AM**
Page 43: [9] Deleted	**Seoung Soo Lee**	**8/27/19 7:46:00 AM**
Page 43: [10] Deleted	**Seoung Soo Lee**	**8/28/19 7:19:00 AM**
Page 44: [11] Deleted	**Seoung Soo Lee**	**8/27/19 7:26:00 AM**
Page 44: [12] Deleted	**Seoung Soo Lee**	**8/28/19 7:20:00 AM**
Page 44: [13] Deleted	**Seoung Soo Lee**	**8/28/19 7:21:00 AM**
Page 44: [14] Deleted	**Seoung Soo Lee**	**8/28/19 7:22:00 AM**
Page 44: [15] Deleted	**Seoung Soo Lee**	**8/28/19 7:22:00 AM**
Page 44: [16] Deleted	**Seoung Soo Lee**	**8/27/19 7:27:00 AM**

Page 61: [17] Deleted	**Seoung Soo Lee**	**8/4/19 7:28:00 AM**
Page 61: [18] Deleted	**Seoung Soo Lee**	**7/30/19 7:37:00 AM**
Page 61: [19] Deleted	**Seoung Soo Lee**	**7/30/19 8:02:00 AM**
Page 61: [20] Deleted	**Seoung Soo Lee**	**8/4/19 7:24:00 AM**
Page 69: [21] Deleted	**Seoung Soo Lee**	**8/4/19 7:18:00 AM**